Synthesis and Biological Evaluation of Arylamide Sulphonate Derivatives as Ectonucleotide Pyrophosphatase/Phosphodiesterase-1 and -3 Inhibitors

Saif Ullah, Julie Pelletier, Jean Sévigny, and Jamshed Iqbal*

Read Online

ACCESS | Metrics & More | Article Recommendations | SI Supporting Information

ABSTRACT: Aberrant level of ectonucleotide pyrophosphatase/phosphodiesterase-1 and -3 is linked with numerous disorders, for instance, diabetes, cancer, osteoarthritis, chondrocalcinosis, and allergic reactions. These disorders may be cured or minimized by blocking the activity of ENPP1 and ENPP3 isozymes. In this study, arylamide sulphonates were synthesized, characterized, and evaluated for their capability to affect the activity of isozymes ENPP1 and ENPP3. Among the selective inhibitors of ENPP1, compounds **4f** and **4q** exhibited sub-micromolar IC_{50} values of 0.28 ± 0.08 and 0.37 ± 0.03 μM, respectively, followed by **7a**, with IC_{50} equal to 0.81 ± 0.05 μM, whereas out of the selective inhibitors of isozyme ENPP3, **4t** and **7d** preferably lessened the activity to half of the maximal inhibitory concentration of $0.15 \pm$

0.04 and 0.16 ± 0.01 μM alternatively. In addition, many structures including **4c, 4g, 4k, 4l, 4n, 4o, 4r, 4s, 7b, 7c**, and **7e** inhibited the activity of both isozymes to a significant level. Enzyme kinetic study of compound **4j** revealed an uncompetitive mode of inhibition of ENPP1 isozyme, while **7e** competitively blocked the activity of ENPP3. Cell viability analysis revealed the compound **4o** as a cytotoxic agent against MCF7 (human breast cancer cell line) with a percentage inhibition of $63.2 \pm 2.51\%$, whereas compounds **4c, 4d, 4n**, and **7d** decreased the HeLa cell viability (human cervical cancer cell line) to more than 50%. The tested compounds were non-cytotoxic against HEK293 (a human embryonic kidney cell line). Molecular docking analysis of selected inhibitors of both isozymes produced optimistic interactions with the influential amino acids, such as Leu290, Lys295, Tyr340, Asp376, His380, and Pro323 of ENPP1, whereas residues Asn226, His329, Leu239, Tyr289, Pro272, Tyr320, and Ala205 of ENPP3 crystallographic structure formed interactions with the potent inhibitors.
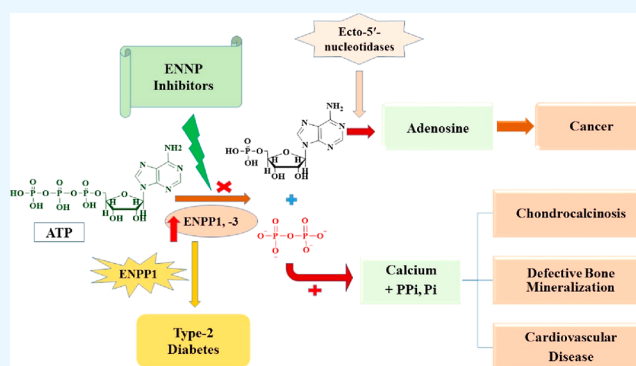
1. INTRODUCTION

The members of the ENPP family are conserved and ubiquitous eukaryotic enzymes with an extracellular active site and exist as membrane-bounded glycoproteins.[1] The ENPP family contains seven fundamental isozymes (ENPP1−7), which are numbered as per their cloning order.[2] ENPP1, ENPP2, ENPP3, and ENPP4 can hydrolyze a variety of nucleotides together with dinucleoside polyphosphates, nucleotide sugars, and cyclic (di-)nucleotides and release corresponding nucleoside 5′-mono-phosphates; for example, ATP is hydrolyzed into AMP and pyrophosphate (PPi).[3] However, among the nucleotide hydro-lyzing potential of isozymes (ENPP1, ENPP2, ENPP3, and ENPP4), the nucleotide metabolizing activity of ENPP2 is weak. ENPP2 prefers phospholipids as a substrate, whereas ENPP6 and ENPP7 are alkaline sphingomyelinases; hence, instead of nucleotidases, the subtypes (ENPP2, ENPP6, and ENPP7) may be identified as phospholipases.[4−8]

ENPP1 was initially found as the surface sign for B-lymphocytes that secrete antibodies; therefore, it was named plasma-cell differentiation antigen-1 or PC-1.[9] ENPP1 exists in

several tissues such as in the bone (osteoblast) and cartilage (chondrocytes), where it performs an essential part in the mineralization process.[10] ENPP1 is the transmembrane glycoprotein of homodimeric type II, accompanied by an N-terminal transmembrane domain, a catalytic domain, a C-terminal nuclease-like domain, and two somatomedin-B-like domains.[11] The subcellular location of ENPP1 is determined by the transmembrane domain, which is essential for the dimerization of monomers by multiple disulfide bonds. It is also noteworthy that the SMB2 domain of the ENPP1 is assumed to be the residue for the insulin receptor interaction. The ENPP1 catalytic domain amino acid residues make 24−60% likeness among the various isozymes of other human
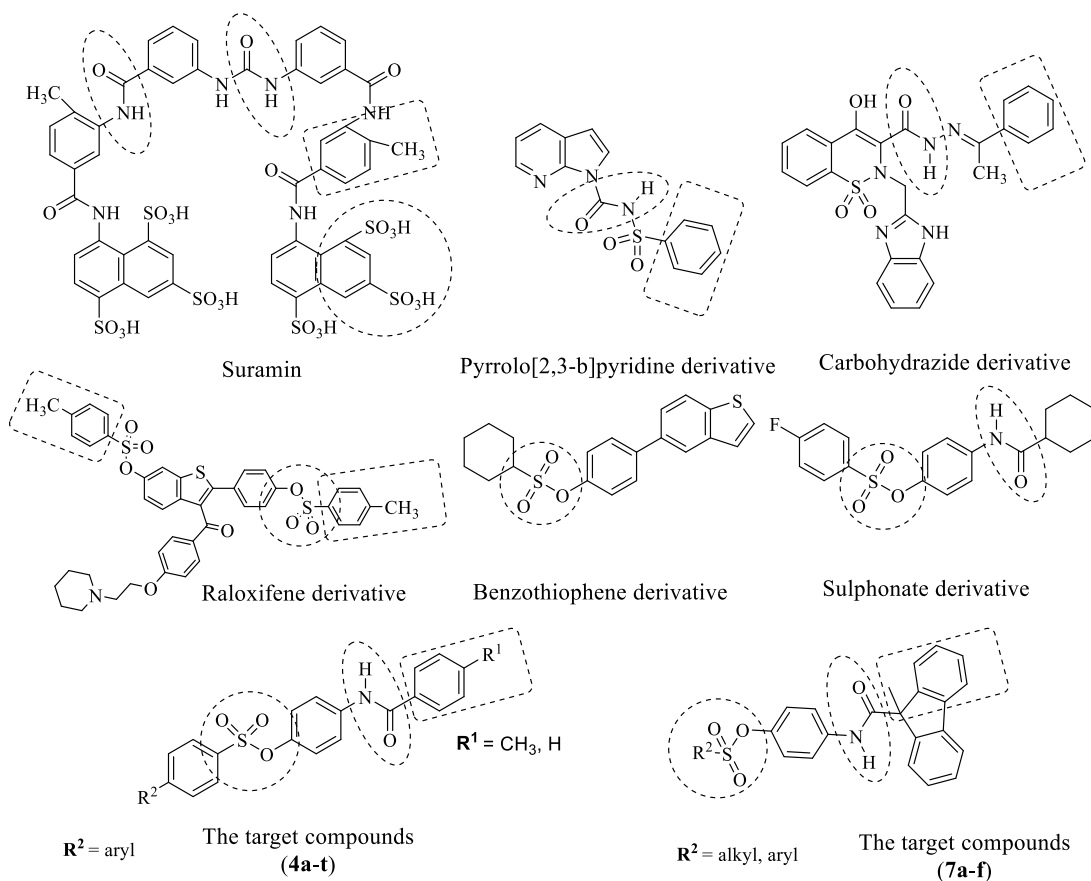
Figure 1. Previously reported structures of ENPP inhibitors and the target compounds.

ENPPs (ENPP2−7) and similarity to the alkaline phosphatase family (APs).[12] Like the APs, two Zn^{2+} cations are strongly linked by six preserved Asp/His residues at the active site. In addition, the nuclease-like domain is connected to the catalytic domain via a linker region called the "lasso loop".[13] If any mutation occurs in this linker region, the catalytic activity of the isozyme is eliminated. The nuclease-like domain does not itself reveal catalytic activity, but it is required to translocate ENPPs from the endoplasmic reticulum to the Golgi apparatus, necessary for the correct folding of the ENPPs. Moreover, this domain includes a perceived "EF hand" Ca^{2+} binding motif, which is significant for the catalytic activity of ENPP1. Though PPi is essential for the prevention of ectopic mineralization, its over-supply contributes to the mineral aggregation of calcium pyrophosphate dihydrate (CPPD) in joints. This situation is usually associated with age-related osteoarthritis, known as chondrocalcinosis. The role of ENPP1 was also found for insulin receptor signaling. The over-expression of ENPP1 was found to be linked with defective insulin-stimulated autophosphorylation in patients with type 2 diabetes. Moreover, ENPP1 was also identified and associated with tumor gradation in human astrocytic brain tumors.[14]

The isozyme ENPP3 (a glycoprotein) is associated with the plasma membrane of the cell. ENPP3 (CD203c) is expressed on surfaces of various body organs such as epithelial and mucosal, particularly on mast cells and basophils.[15−17] ENPP3 is actively involved in fluid homeostasis, modulation of bile formation, and cerebral spinal fluid secretion. ENPP3 is actively involved against the synchronization of nucleotide sugar glycosylation of brain-specific proteins and involves intracellular as well as

extracellular polyphosphate hydrolysis. The molecular structure of ENPP3 contains parallel β-sheets of eight trapped catalytic phosphodiesterase (PDE) domain in the molecular structure of ENPP3 that hold five active N-glycosylation sites and eight α-helices on each side, representing a major component of alkaline phosphatase superfamily.[12,18] This PDE domain is linked to the nuclease-like region (NUC) through the linker L2, two somatomedin B (SMB1 and SMB2 domains) with the L1 link attached to the NUC.[19] An elevated proportion of ENPP3 on the cell surface was detected in comparison to other inflammatory mediators, which stimulated basophils with antigen-bound IgE. ATP emissions are thus impaired by ENPP3 and served as a sign of recognition that basophils of patients have allergic responsiveness.[20]

Several structures with sulphonate moiety are reported to possess therapeutic importance such as suramin (Figure 1) with a complex structure and poly sulphonate groups, being widely used as a positive control of choice in different biological studies.[21] In the previous study, we have reported pyrrolo[2,3-b]pyridine derivatives such as (N-(pyrrolo[2,3-b]pyridine-1-carbonyl)benzenesulfonamide), which was found as a selective inhibitor of ENPP1 with an IC_{50} value of 4.50 ± 0.16 μM and carbohydrazide-based derivative, which selectively blocked the activity of ENPP3 to half of the maximal value of 0.15 μM.[22,23] Various previously reported structures with sulphonate scaffolds including raloxifene sulphonates, benzofuran, and benzothiophene sulphonates exhibited significant enzyme inhibitory activity to sub-micromolar levels, for example, raloxifene sulphonate derivative 3-(4-(2-(piperidin-1-yl)ethoxy)benzoyl)-2-(4-(tosyloxy)phenyl)benzo[b]thiophen-6-yl-4-methylbenze-
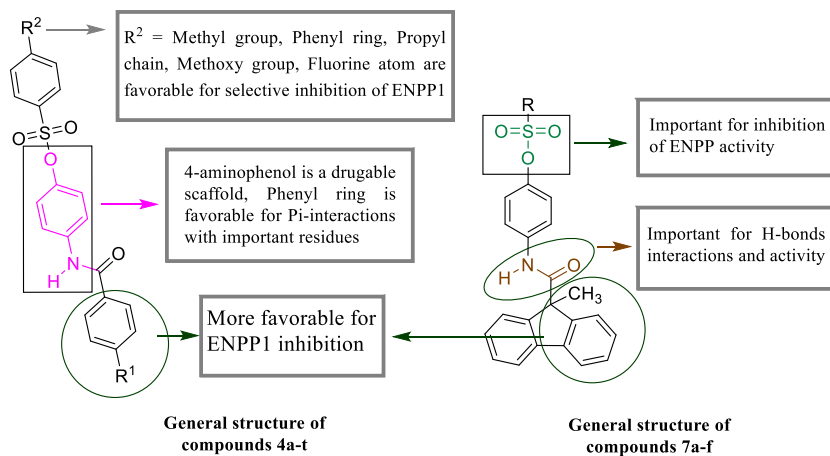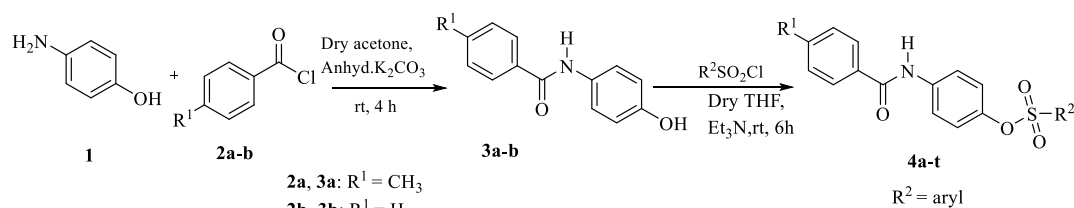
Figure 2. Structure—activity relationship of the designed compounds.

Scheme 1. Synthesis of Sulphonate Derivatives (4a−t)

2a, **3a**: $R^1 = CH_3$
2b, **3b**: $R^1 = H$

4a : $R^1 = CH_3$; $R^2 = 4\text{-Me}(C_6H_4)$
4b : $R^1 = CH_3$; $R^2 = \text{Phenyl}$
4c : $R^1 = CH_3$; $R^2 = 4\text{-I}(C_6H_4)$
4d : $R^1 = CH_3$; $R^2 = 4\text{-OCH}_3(C_6H_4)$
4e : $R^1 = CH_3$; $R^2 = 4\text{-Cl}(C_6H_4)$
4f : $R^1 = CH_3$; $R^2 = 4\text{-}n\text{-propyl}(C_6H_4)$
4g : $R^1 = CH_3$; $R^2 = 4\text{-OCF}_3(C_6H_4)$
4h : $R^1 = CH_3$; $R^2 = \text{Biphenyl}$
4i : $R^1 = CH_3$; $R^2 = CH_2(C_6H_4)$
4j : $R^1 = CH_3$; $R^2 = 4\text{-}n\text{-butyl}(C_6H_4)$

4k : $R^1 = CH_3$; $R^2 = 4\text{-F}(C_6H_4)$
4l : $R^1 = CH_3$; $R^2 = 2\text{-F}(C_6H_4)$
4m : $R^1 = H$; $R^2 = 4\text{-OCH}_3(C_6H_4)$
4n : $R^1 = H$; $R^2 = CH_2(C_6H_4)$
4o : $R^1 = H$; $R^2 = 4\text{-}n\text{-propyl}(C_6H_4)$
4p : $R^1 = H$; $R^2 = \text{Biphenyl}$
4q : $R^1 = H$; $R^2 = 8\text{-quinolinyl}$
4r : $R^1 = H$; $R^2 = 4\text{-I}(C_6H_4)$
4s : $R^1 = H$; $R^2 = 4\text{-F}(C_6H_4)$
4t : $R^1 = H$; $R^2 = 4\text{-OCF}_3(C_6H_4)$

Scheme 2. Synthesis of Sulphonate Derivatives (7a−f)

7a : $R = 2\text{-F}(C_6H_4)$
7b : $R = CF_3$
7c : $R = 4\text{-F}(C_6H_4)$

7d : $R = \text{Methyl}$
7e : $R = 4\text{-CH}_3(C_6H_4)$
7f : $R = \text{Phenyl}$
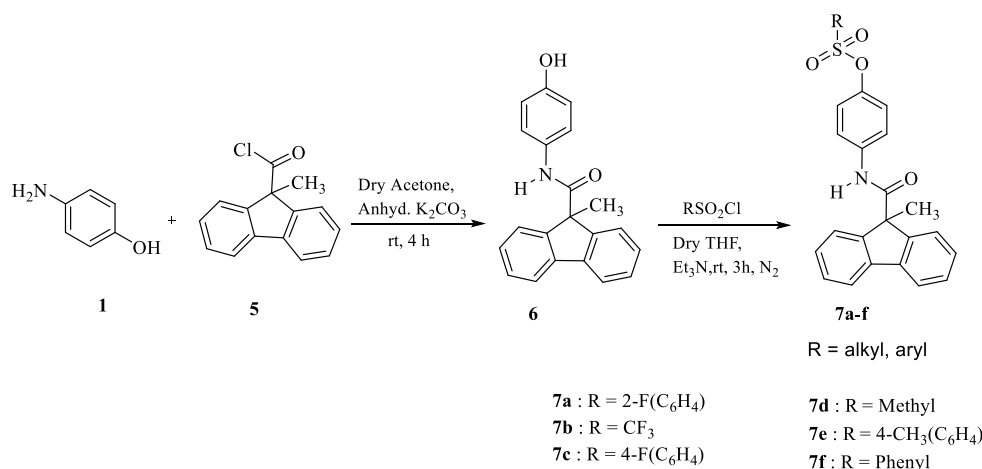
nesulfonate tabulated selective inhibition of isozyme ENPP1 to an IC_{50} value of 0.45 μM, and benzothiophene derivative (4-(benzo[b]thiophen-5-yl)phenyl cyclohexanesulfonate) was endowed with $IC_{50} = 0.12$ μM against ENPP1 and 1.89 μM toward ENPP3.[24,25] We have also reported sulphonate derivatives mainly based on non-aromatic or saturated cyclic hydrocarbons.

These structures exhibited considerable inhibitory activity but limited preferable selectivity among the three isozymes ENPP1, ENPP2, and ENPP3.[26]

The selected structural determinants in the target compounds are deemed unique scaffolds due to their importance in medicinal chemistry (Figure 2). The compounds with

carboxamide moiety have been reported as antimycobacterial agents and antibacterial drugs.[27−31] The compounds bearing the sulphonate and sulphamoyl group have shown anticancer, anti-hyperglycemic, and antimicrotubule properties.[32−35] Similarly, 4-aminophenol has been reported as a pharmacophore of the drug "Paracetamol".[36] Considering the importance of the structural scaffolds of the reported structures such as the carboxamide moiety, sulphonate group, and 4-aminophenol, we moved toward the synthesis of arylamide-based sulphonates. The combination of various structural components referred to the compound as multiple choices of selectivity toward isozymes ENPP1 and ENPP3.

2. RESULTS AND DISCUSSION

2.1. Chemistry. The synthetic pathways to design arylamide sulphonate derivatives **4a−t** and **7a−f** are illustrated in Schemes 1 and 2, respectively. The required sulphonate derivatives (**4a−t**) were synthesized by a 2-step synthetic pathway. In the first step, the base-catalyzed nucleophilic-electrophilic substitution reaction of 4-aminophenol (**1**) with 4-methyl benzoyl chloride (**2a**) or benzoyl chloride (**2b**) led to the formation of structure **3a** or **3b**, respectively. In the second step, sulphonate derivatives **4a−l** were produced by treating **3a** with substituted benzene sulfonyl chloride; similarly, sulphonate derivatives from **4m** to **4t** were obtained by reaction of **3b** with substituted benzene sulphonate chlorides under the same conditions. The second series of sulphonate derivatives (**7a−f**) were synthesized by a reaction of **1** with 9-methyl-9H-fluorene-9-carbonyl chloride (**5**) to yield the phenolic intermediate **6**, which was further used with various sulfonyl chlorides to get the final products.

2.2. Enzyme Inhibition Assay. The enzymatic inhibitory potential of the synthesized molecules was determined against the hydrolytic activity of ENPP1 and ENPP3 isozymes. A number of compounds manifested selective and significant inhibition of the activity of both isozymes. The results of the enzymatic evaluation of the compounds **4a−t** and **7a−f** are depicted in Tables 1 and 2, respectively.

2.3. Study of Structure−Activity Relationship of Compounds Measured through Enzyme Inhibition Assay. The effect of different structural variations at position "R^1, R^2" for compounds **4a−t** and **7a−f** was studied in terms of the structure−activity relationship. Comparison of results of compounds **4a**, **4b**, **4f**, and **4j** by the structures indexed interesting results. Compound **4a** with 4-methyl phenyl linkage inhibited both isozymes' activity to a lesser extent, merely 26.2% in the case of ENPP1 and only 17.0% for ENPP3. These results were slightly modified when the p-methyl group was removed with the phenyl ring only (**4b**). Again structure **4b** was devoid of ENPP1 inhibitory potential but blocked the activity of ENPP3 to an IC$_{50}$ value of 29.76 ± 2.13 μM. Modification of phenyl ring substitution to 4-methoxy phenyl group (**4d**) inversed the inhibitory potential more selectively to ENPP1 (IC$_{50}$ = 0.18 ± 0.01 μM) and blocked the ENPP3 isozyme to only 45.7%.

In compliance with the modification at phenyl ring with methyl linkage, elongation of this linkage to three carbons atoms (**4f**) and four carbon atoms (**4j**) significantly and selectively turned the activity toward ENPP1, that is, compound **4f** with a propyl linkage blocked the ENPP1 to IC$_{50}$ = 0.28 ± 0.08 μM, whereas **4j** with a butyl linker inhibited the isozyme ENPP1 with an IC$_{50}$ value of 0.23 ± 0.03 μM. These three structures with hydrocarbon linkers (**4d**, **4f**, **4j**) poorly blocked the hydrolytic activity of ENPP3 to very low or nearly 50% percent inhibition values such as 45.7, 8.4, and 42.1%, respectively. The outcomes

Table 1. ENPP1 and ENPP3 Isozyme Inhibition at 100 μM Compound Concentration, Presented in IC$_{50}$ ± SEM (μM) Values or Percentage Inhibition ±SD

| codes | R^1 | R^2 | IC$_{50}$ ± SEM (μM)[a] or % inhibition ± SD[b] | |
			ENPP1	ENPP3
4a	CH$_3$	4-Me(C$_6$H$_4$)	26.2 ± 2.11[b]	17.0 ± 3.24[b]
4b	CH$_3$	phenyl	45.2 ± 1.53[b]	29.8 ± 2.11[a]
4c	CH$_3$	4-I(C$_6$H$_4$)	14.41 ± 0.54[a]	4.23 ± 0.38[a]
4d	CH$_3$	4-OCH$_3$(C$_6$H$_4$)	0.18 ± 0.01[a]	45.7 ± 2.35[b]
4e	CH$_3$	4-Cl(C$_6$H$_4$)	44.8 ± 1.52[b]	0.82 ± 0.12[a]
4f	CH$_3$	4-n-propyl(C$_6$H$_4$)	0.28 ± 0.08[a]	8.4 ± 3.11[b]
4g	CH$_3$	4-OCF$_3$(C$_6$H$_4$)	0.45 ± 0.07[a]	0.19 ± 0.02[a]
4h	CH$_3$	biphenyl	1.73 ± 0.03[a]	27.1 ± 4.54[b]
4i	CH$_3$	CH$_2$(C$_6$H$_4$)	0.13 ± 0.01[a]	46.7 ± 1.54[b]
4j	CH$_3$	4-n-butyl(C$_6$H$_4$)	0.23 ± 0.03[a]	42.1 ± 3.43[b]
4k	CH$_3$	4-F(C$_6$H$_4$)	7.61 ± 0.02[a]	0.37 ± 0.08[a]
4l	CH$_3$	2-F(C$_6$H$_4$)	0.15 ± 0.01[a]	3.48 ± 0.34[a]
4m	H	4-OCH$_3$(C$_6$H$_4$)	0.82 ± 0.05[a]	22.6 ± 2.12[b]
4n	H	CH$_2$(C6H4)	3.96 ± 0.12[a]	4.12 ± 0.05[a]
4o	H	4-n-propyl(C$_6$H$_4$)	1.71 ± 0.04[a]	2.12 ± 0.08[a]
4p	H	biphenyl	1.51 ± 0.02[a]	33.5 ± 1.92[b]
4q	H	8-quinolinyl	0.37 ± 0.03[a]	19.5 ± 3.53[b]
4r	H	4-I(C$_6$H$_4$)	2.01 ± 0.34[a]	0.53 ± 0.19[a]
4s	H	4-F(C$_6$H$_4$)	5.76 ± 0.57[a]	2.95 ± 0.25[a]
4t	H	4-OCF$_3$(C$_6$H$_4$)	41.4 ± 3.24[b]	0.15 ± 0.04[a]
Suramin			7.80 ± 0.09[a]	0.89 ± 0.16[a]

[a]The results are obtained by means of a triplicate assay; IC$_{50}$ values are calculated for compounds showing inhibition of enzyme activity to more than 50%; SEM = standard error mean. [b]Percentage inhibition of the compounds exhibiting <50% inhibition; SD = standard deviation.

Table 2. ENPP1 and ENPP3 Isozyme Inhibition at 100 μM Compound Concentration, Presented in IC$_{50}$ ± SEM (μM) Values or %Age Inhibition ±SD

| codes | R | IC$_{50}$ ± SEM (μM)[a] or % inhibition ± SD[b] | |
		ENPP1	ENPP3
7a	2-F(C$_6$H$_4$)	0.81 ± 0.05[a]	28.2 ± 3.22[b]
7b	CF$_3$	0.90 ± 0.16[a]	4.16 ± 0.22[a]
7c	4-F(C$_6$H$_4$)	0.50 ± 0.03[a]	6.69 ± 1.89[a]
7d	methyl	9.2 ± 4.13[b]	0.16 ± 0.01[a]
7e	4-CH$_3$(C$_6$H$_4$)	18.87 ± 0.54[a]	0.38 ± 0.13[a]
7f	phenyl	8.45 ± 0.25[a]	42.1 ± 2.44[b]

[a]The results are obtained by means of a triplicate assay; IC$_{50}$ values are calculated for compounds showing inhibition of enzyme activity to more than 50%; SEM = standard error mean. [b]Percentage inhibition of the compounds exhibiting <50% inhibition; SD = standard deviation.

of **4d**, **4f**, and **4j** suggested that the methoxy group or long hydrocarbon side chain with the phenyl ring was favorable to ENPP1 inhibition. A study of SAR for compounds **4b** and **4h** showed selective but opposite behavior toward isozymes ENPP1 and ENPP3. The molecule with a single phenyl ring attachment at position "R^2" possessed the selective potential to ENPP3, whereas the biphenyl attachment at the same position turned the selectivity more specifically to isozyme ENPP1. The structures possessing halogens with phenyl moiety produced variable but promising outcomes. Comparison of SAR for **4c**, **4e**, and **4k** substituted with 4-iodophenyl, 4-chlorophenyl, and 4-fluoro-phenyl at the "R^1" position showed almost non-selective
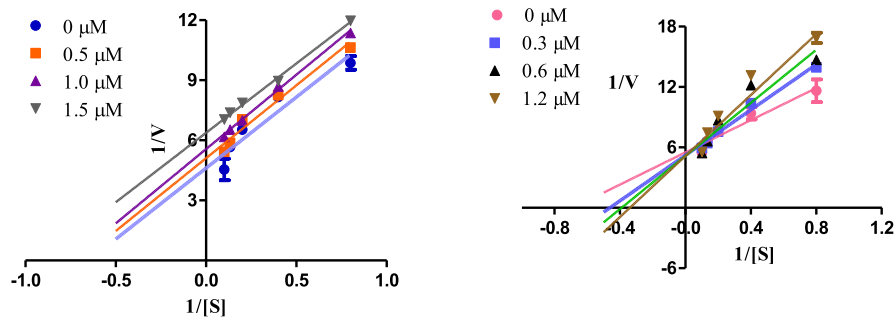
Figure 3. Presentation of Lineweaver−Burk plots of enzyme kinetics of **4j** (left) and **7e** (right). The experiments were performed in triplicates.

Table 3. Cytotoxicity of 100 μM Compound on MCF7, HeLa, and HEK293 Cell Lines

codes	MCF7 (% inhibition ±SD)[a]	HeLa cell line (% inhibition ±SD)[a]	HEK293 (% inhibition ±SD)[a]
4a	1.1 ± 0.12	16.4 ± 0.92	5.3 ± 0.81
4b	7.4 ± 0.04	44.9 ± 1.81	6.4 ± 0.22
4c	33.2 ± 1.32	57.8 ± 2.72	15.2 ± 0.83
4d	31.5 ± 2.43	53.4 ± 1.93	13.1 ± 0.73
4e	24.2 ± 1.73	32.4 ± 3.82	8.3 ± 0.35
4f	25.7 ± 0.92	49.2 ± 2.12	4.2 ± 0.12
4g	11.7 ± 0.84	17.7 ± 0.72	3.2 ± 0.11
4h	9.1 ± 0.71	48.2 ± 1.43	4.8 ± 0.24
4i	5.7 ± 0.06	38.5 ± 1.14	11.2 ± 0.92
4j	13.3 ± 0.73	19.1 ± 1.11	27.6 ± 2.55
4k	11.2 ± 0.52	7.7 ± 0.73	2.1 ± 1.22
4l	0.5 ± 0.03	14.3 ± 3.52	17.4 ± 0.83
4m	4.1 ± 0.01	7.1 ± 0.81	2.3 ± 1.12
4n	7.3 ± 0.03	51.3 ± 0.82	5.8 ± 0.23
4o	63.2 ± 2.51	38.7 ± 2.43	12.6 ± 0.74
4p	8.4 ± 0.75	5.3 ± 0.07	4.3 ± 0.15
4q	11.2 ± 1.04	24.2 ± 1.44	4.6 ± 0.32
4r	10.2 ± 0.86	12.6 ± 0.73	11.3 ± 0.71
4s	2.1 ± 0.08	16.5 ± 1.12	20.6 ± 1.14
4t	29.6 ± 1.22	49.7 ± 2.53	8.6 ± 0.14
7a	12.7 ± 0.62	10.7 ± 0.72	14.6 ± 1.12
7b	14.1 ± 0.63	32.4 ± 2.63	24.5 ± 1.16
7c	12.4 ± 1.22	23.5 ± 1.64	9.2 ± 0.42
7d	0.2 ± 0.06	56.3 ± 1.17	5.5 ± 0.36
7e	0.3 ± 0.15	33.8 ± 1.56	12.4 ± 1.42
7f	5.6 ± 1.11	28.1 ± 1.33	6.2 ± 1.17
cisplatin	N.D	84.3 ± 2.72	65.5 ± 1.48
doxorubicin	88.8 ± 2.74	N.D	N.D

[a]Cytotoxicity of compounds at 100 μM, calculated by taking a mean of the triplicate assays; % inhibition ± standard deviation; ND = not determined.

behavior without significant inhibitory difference among the two isozymes, except inhibitor **4e**, which exhibited comparatively more affinity for ENPP3 with IC$_{50}$ equal to 0.82 ± 0.12 μM. The relative study of SAR of **4k** and **4l** revealed that the presence of fluorine atom at the para position was much favorable for ENPP3, whereas fluorine atom at the meta position shifted the potency toward ENPP1.

The presence of the methoxy group on the phenyl ring rendered compound **4m** toward the selectivity of ENPP1 (IC$_{50}$ = 0.82 ± 0.05 μM). The same selectivity pattern was observed in the case of **4p** with biphenyl attachment at the R^2 position, reducing the activity of ENPP1 to half of the maximal inhibitory concentration (IC$_{50}$) of 1.51 ± 0.02 μM and only 33.5% inhibition to ENPP3 isozyme. This pattern of selectivity suggested the −OCH$_3$ or phenyl group linkage at the phenyl ring, which was favorable for ENPP1 inhibition. Elongation of

the side chain to three carbon atoms (**4o**) abolished the selectivity pattern for either of the isozymes. A careful comparative study of structures **4f** and **4o** highlighted the point that the *n*-propyl linkage is much beneficial toward the selective inhibition of ENPP1 activity in the presence of methyl group on the other side of the structure. The presence of 8-quinolinyl moiety produced the most potent and selective structure (**4q**) that blocked the ENPP1 activity to IC$_{50}$ value equal to 0.37 ± 0.03 μM, suggesting the heterocyclic attachment favorable for the inhibition of ENPP1 isozyme activity. The halogenated structures **4r−t** revealed compound **4t** possessing −OCF$_3$ as a selective inhibitor for ENPP3 (0.15 ± 0.04 μM), contributing to the effect of −OCF3 toward inhibition of ENPP3 isozyme activity. Moreover, the methoxy group substitution was found preferable for only ENPP1 (**4d**, **4m**), and the results of **4h** and **4p** demonstrated selective behavior

toward ENPP1, suggesting the importance of the biphenyl group for ENPP1 inhibition (Table 1).

In the next series of compounds (**7a−f**), aromatic and aliphatic sulfonyl chlorides were used to produce complex but promising structures. Interestingly, among the six compounds (**7a−f**), two compounds selectively blocked the activity of ENPP1, **7a** with 2-fluorophenyl substitution (IC$_{50}$ = 0.81 ± 0.05 μM) and **7f** (IC$_{50}$ = 8.45 ± 0.25 μM) possessing a single phenyl ring at position "R", and the molecule **7d** carrying a methyl group preferably inhibited the isozyme ENPP3 illustrating an IC$_{50}$ value of 0.16 ± 0.01 μM. The trifluoromethane substitution produced structure **7b**, which presented dual inhibition of both isozymes (ENPP1, IC$_{50}$ = 0.90 ± 0.16 μM; ENPP3, IC$_{50}$ = 4.16 ± 0.22 μM), whereas a single fluorine atom as a 4-fluorophenyl attachment preferably blocked the ENPP1 activity over ENPP3.

2.4. Pattern of Enzyme Inhibition of Compounds 4j and 7e. The pattern of enzyme inhibition for a single active compound against each isozyme was assessed by constructing the Lineweaver−Burk graphs (Figure 3). The mode of inhibition for the comparatively selective and potent inhibitor of ENPP1 (**4j**) and ENPP3 (**7e**) was determined by performing enzyme kinetic studies. Compound **4j** blocked ENPP1 uncompetitively, whereas **7e** competitively inhibited ENPP3 activity.

2.5. Cell Cytotoxicity Analysis (MTT Assay). The MTT [3-(4,5-dimethylthiazol-2-yl)-2,5-diphenyltetrazolium bromide] assay was executed to find out the cytotoxic effect of the compounds on human breast cancer cell line (MCF7), human cervical cancer cell line (HeLa), and human embryonic kidney cell line (HEK293). The compounds were found cytotoxic against cancer cell lines, but none of the molecules were toxic on normal cell lines. The results of the cytotoxicity assay are tabulated in Table 3. The cytotoxic potential of the compounds was evaluated on the three cancerous cell lines: (1) MCF7, a human breast cancer cell line; (2) HeLa, a human cervical cancer cell line; and (3) HEK293, a human embryonic kidney cell line. Neither of the tested compounds manifested a significant effect on MCF7 cancer cell viability except for **4o** with 63.2% inhibition checked at 100 μM compound concentration. The molecules **4c**, **4d**, **4n**, and **7d** decreased the viability of HeLa cancer cells to above 50%. None of the compounds affected the viability of normal cell lines to a significant level.

2.6. Molecular Docking Studies. The putative mode of structural component's interaction with the amino acid residues of ENPP1 and ENPP3 isozymes was found by applying molecular docking analysis. The in silico findings produce reliable outcomes following the in vitro results. The 2D and 3D modes of interaction are shown in Figures 4−8.

2.6.1. Molecular Docking Studies at the Crystal Structure of ENPP1 Isozyme. The most active synthesized compounds were consigned to molecular docking analysis to elaborate the inhibitory results against the ENPP1 isozyme. The reported crystallographic structure of human ENPP1, docked with reference ligand "N-{4-[(7-methoxyquinolin-4-yl)oxy]phenyl}-sulfuric diamide" (TZV), was downloaded from Protein Data Bank (PDB) with PDB ID = 6wew.[37] The bound ligand TZV was found in contact with several amino acid residues of the catalytic site; such as the quinoline nucleus was stacked between Tyr340 and Phe257 and through π−π T-shaped interaction with Pro323 and Leu290. Moreover, TZV showed H-bond interaction with Lys338, Lys295, Asp376, and His380. A π-alkyl and π-anion connection was found with Leu290, Pro323, and Asp218.[37] The most selective and relatively potent inhibitor
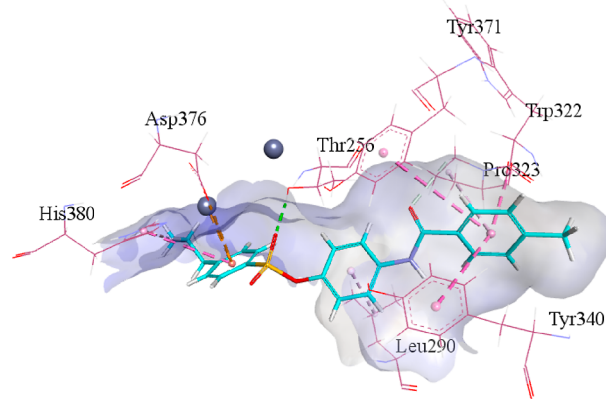

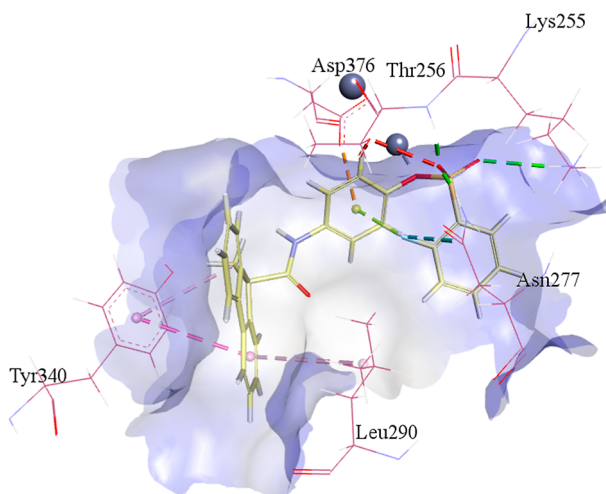**Figure 4.** Illustration of 3D plausible binding modes for selective inhibitor **4f** with ENPP1 isozyme.

Figure 5. Illustration of 3D binding interactions of selective inhibitor **7a** with residues of ENPP1 isozyme.
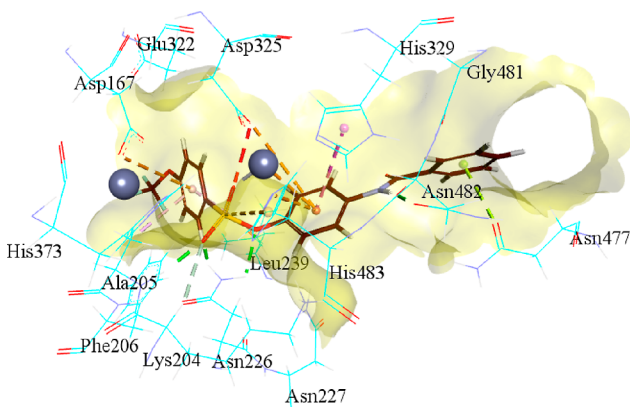
Figure 6. Presentation of 3D binding modes of inhibitor **4t** with ENPP3 isozyme residues.

of ENPP1 **4f** showed H-bonding linkage between the oxygen atom of sulphonate group and amino acid residue Thr256. The inhibitor **4f** rested itself through an array of π-linkages, that is, π−π stacked, π−π T-shaped, amide-π stacked, and π-alkyl bonds with residues His380, Tyr371, Tyr340, Trp322, and Leu290. Moreover, **4f** was coordinated to zinc metal ion, Asp376, through π-anion and π-cation bonds (Figure 4).
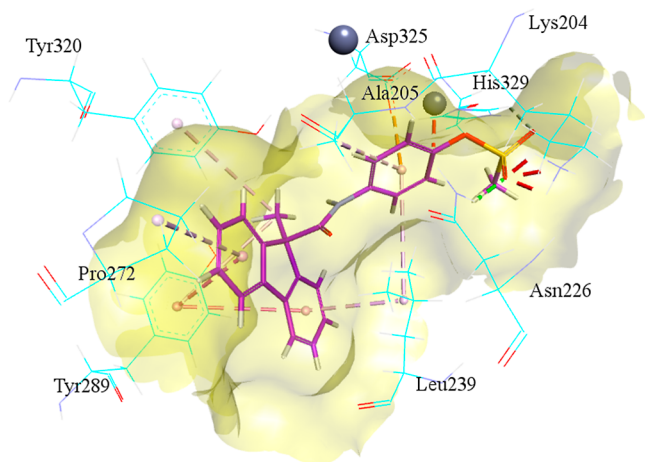
Figure 7. Illustration of 3D binding modes of inhibitor **7d** with ENPP3 isozyme residues.

The docking studies of another selective inhibitor of isozyme ENPP1 (**7a**) manifested a wide range of occupancy of amino acids, attributing to its selectivity. Residues Lys255, Asn277, and

Thr256 coordinated through hydrogen bonds, predominately with sulphonate group of **7a**. Similar to **4f**, compound **7a** stabilized itself via π-connections such as a π-anion link to Asp376, π−π stacked connection Tyr340, π-alkyl interaction to residues Leu290, and Tyr340. Moreover, Zn^{2+} chelation connected to the oxygen atom of sulphonate moiety was observed as depicted in Figure 5.

2.6.2. Molecular Docking Studies at the Crystal Structure of ENPP3 Isozyme. The selective inhibitor of ENPP3 **4t** stabilized itself through an array of several amino acid residues. H-bond interactions were observed between oxygen atoms of sulphonate group and residues Ala205, Asn226, and Lys204 and hydrogen of amide moiety and residue Asn482. Several π-interactions contributed to the stability and activity of **4t** in the active site. These linkages include π-anion connection with Asp167: π-alkyl stick bridging Ala205; Leu239: π−π stacked connection with His329: π-sulfur attachment with His483: π-anion linkage with His483; and Asp167: π-lone pair link among the lone pair of asparagine residue (Asn477) and phenyl ring of phenyl acetamide moiety. A π-cation linkage was noticed between the zinc ion and sulphonate group oxygen. More noticeably, an unfavorable bond was observed among Asp325
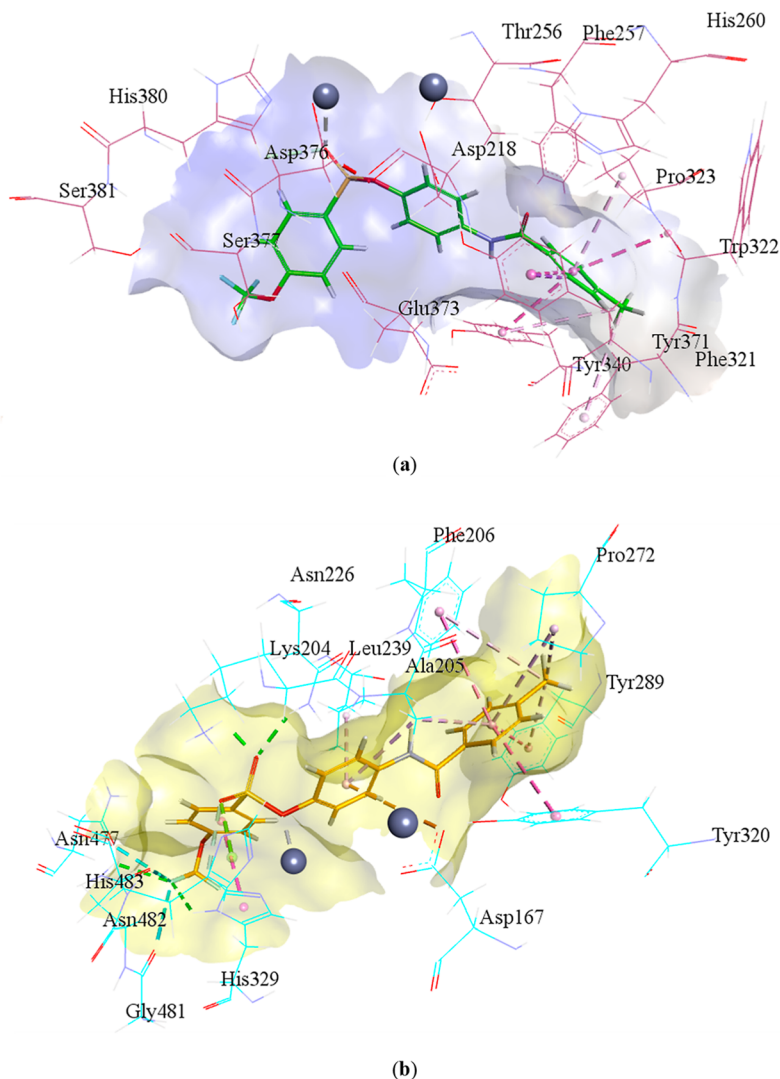

(a)

(b)

Figure 8. Presentation of 3D binding interaction of dual inhibitor **4g**; (a) 3D binding modes with ENPP1 and (b) 3D binding modes with an ENPP3 crystallographic structure.

and oxygen atoms of sulphonate moiety, contributing to the high affinity and stability of the molecule **4t** (Figure 6).

The molecular docking study of another selective structure for ENPP3 (**7d**) revealed promising interactions with amino acid residues. The structure **7d** balanced itself through hydrogen bonding of sulphonate group oxygens with Asn226 and His329. The three aromatic rings and the methyl group connected to the heterocyclic scaffold formed an array of $\pi-\pi$ stacked and π-alkyl linkages with residues Tyr289, Pro272, Leu239, Tyr320, and Ala205. In addition, one π-anion interaction was found between the phenyl ring of phenyl methanesulfonate attachment and Asp325 as shown in Figure 7.

2.6.3. Molecular Docking Studies at the Crystal Structure of ENPP1 and ENPP3 Isozymes. The observation of the plausible binding mode of the relatively potent but dual inhibitor **4g** gave insights into the binary nature or non-selective behavior of the structure. In the case of ENPP1, inhibitor **4g** formed an array of π-connections; Tyr371 ($\pi-\pi$ stacked, π-sigma bond), Tyr340 ($\pi-\pi$ T shaped), Trp322 ($\pi-\pi$ stacked), and Pro323 and Phe321 (π-alkyl linkage). Similar to inhibitors **4f** and **7a**, compound **4g** was also chelated with zinc metal ions. **4g** blocked the catalytic activity of ENPP3 to a low micromolar level, tabulated as the second active inhibitor to ENPP3 (0.19 ± 0.02 μM). The binding modes gave the results in obedience to experimental data. As a result of docking into the ENPP3 crystalline structure, **4g** was linked via four H-bonds: two with Lys204 and Asn226 through the oxygen of sulphonate scaffold and two with Asn482 and His329. The whole structure was surrounded by P_i-linkages of several amino acid residues such as $\pi-\pi$ bonds with residues Tyr289, Tyr320, Phe206, and His329 and π-alkyl and alkyl bonds with Leu239, Ala205, and Pro272. In addition, the important connections were observed with His483 (π-lone pair bond) and Asp167 (π-anion bond). Zinc ion chelation was also observed through the oxygen atom of the sulphonate group (Figure 8).

3. CONCLUSIONS

A new series of compounds possessing specifically sulphonate group was synthesized, characterized, and examined for the affinity and preference to block the activity of ENPP1 and ENPP3 isozymes of the ectonucleotidase pyrophosphatase/phosphodiesterase (ENPP) family. Among the series, **4a**−**t** compounds **4d**, **4f**, **4h**, **4i**, **4j**, **4m**, **4p**, and **4q** selectively blocked the activity of ENPP1 to less or high preferentially, whereas in the group of structures **7a**−**f**, structure **7a** and **7f** preferably inhibited the activity of ENPP1. Among both series, compounds **4f**, **4h**, **4m**, **4p**, **4q**, and **7a** were found as more potent and particular inhibitors of ENPP1 with IC_{50} values of 0.28 ± 0.08, 1.73 ± 0.03, 0.82 ± 0.05, 1.51 ± 0.02, 0.37 ± 0.03, and 0.81 ± 0.05 μM, alternatively. Similarly, compounds **4b**, **4e**, **4t**, and **7d** showed discriminatory selective behavior for ENPP3 with most active structures **4t** (0.15 ± 0.04 μM) and **7d** (IC_{50} = 0.16 ± 0.01 μM). In the same way, compounds **4c**, **4g**, **4k**, **4l**, **4n**, **4o**, **4r**, **4s**, **7b**, **7c**, and **7e** exhibited dual inhibitory behavior to ENPP1 and ENPP3, particularly **4g** as a more potent structure that tabulated IC_{50} = 0.45 ± 0.07 μM against ENPP1 and IC_{50} = 0.19 ± 0.02 μM toward ENPP3. The cancer cell line (MCF7, HeLa) and normal cell line (HEK293) viability assay revealed that compounds **4c**, **4d**, **4n**, and **7d** were cytotoxic against HeLa cancer cell lines. The structure **4o** significantly decreased the MCF7 cancer cell line viability to 63.2%; however, none of the molecules showed cytotoxicity toward normal cell lines and placed the compounds within a safety profile. The plausible

pattern of interactions of selective and non-selective structures with salient amino acids comprising both proteins ENPP1 and ENPP3 complied with in vitro results. In summation, we found several selective and non-cytotoxic inhibitors for both isozymes ENPP1 and ENPP3. These compounds may be further evaluated as therapeutic agents for the ailments associated with ENPP1 and ENPP3 isozymes.

4. EXPERIMENTAL SECTION

4.1. Reagents, Solvents, and Apparatus. The chemicals and solvents used in this study were obtained from commercial sources. Chemicals were used as such, whereas solvents were dried or distilled where required. ^{1}H NMR and ^{13}C NMR spectra were obtained by a Bruker spectrometer (AV 250, AV 300, and AV 500) in solvents CDCL3 and DMSO. FTIR spectra were detected by an ATR apparatus. The high resonance mass spectra (HRMS) ESI was detected on a device Finnigan MAT 95 XP with an HP-5 capillary column using helium as carrier gas (Thermo Electron Corporation). The melting point of the compounds was obtained with the use of the Büchi apparatus. Column chromatography was carried out by using silica gel 60 A with a mesh size of 60−200. Analytical thin-layer chromatography was performed on silica gel plates (0.20 mm, 60 A), and spots were detected through a UV absorbance lamp 254 nm/366 nm.

4.2. General Procedure of Synthesis. *4.2.1. Synthesis of N-(4-Hydroxyphenyl)-4-methylbenzamide (3a) and N-(4-Hydroxyphenyl)benzamide (3b).* The synthesis of compounds **3a** and **3b** was carried out by treating 4-aminophenol (**1**) (4.12 mmol; 0.450 g) with 4-methyl benzoyl chloride (**2a**) (2.50 mmol; 0.386 g) or benzoyl chloride (**2b**) (2.50 mmol; 0.350 g; 0.423 mL), respectively. The reactants were combined with stirring at 0 °C in acetone (50 mL) in the presence of anhydrous potassium carbonate (3.62 mmol; 0.500 g). After that, the reaction mixture was stirred for 4 h at room temperature and filtered. The filtrate proceeded to dryness, the residue was dissolved in ethyl acetate (40 mL), and extraction was carried out by using dilute HCl (30 mL). The organic layer was separated and washing was performed with a saline solution (2 × 20 mL). The separated organic layer was dried of water molecules by using anhydrous sodium sulfate (Na_2SO_4) and filtered. The organic solvent was evaporated to dryness, and obtained compounds were used for the next step.

4.2.2. Synthesis of Arylamide Sulphonates (4a−l, 4m−t). The targeted compounds **4a**−**l** were synthesized by the reaction of **3a** (0.485 mmol; 0.110 g) with various benzene sulfonyl chloride derivatives (0.985 mmol), and compounds from **4m**−**t** were obtained by treating **3b** (0.485 mmol; 0.103 g) with appropriate benzene sulfonyl derivatives. The separate reactions were performed in dry tetrahydrofuran (THF) (12 mL), and triethylamine (2.10 mmol) was added dropwise to the reaction mixture at 0 °C. Each reaction mixture was stirred at room temperature till completion and quenched up to three times with water and ethyl acetate in equal volumes (3 × 20 mL). The organic layer was dried with anhydrous Na_2SO_4 followed by two times washing with a saline solution (2 × 30 mL), filtered, and subjected to dryness on the rotary evaporator. The crude residue was purified by recrystallization with absolute ethanol.

4.2.2.1. 4-(4-Methylbenzamido)phenyl 4-Methylbenzene-sulfonate (4a). Yield: 74%; colorless solid; mp: 213−216 °C; FT-IR ($\bar{v}$, cm^1, neat): 3352 (N−H, stretching), 2921, 2851 (C−H, stretching), 1652 (C=O, stretching), 1528, 1506, 1343, 1172, 1143, 1092; ^{1}H NMR (300 MHz, DMSO, δ = ppm):

10.26 (s, 1H, CONH), 7.85 (d, J = 8.2 Hz, 2H, Ar–H), 7.74 (dd, J = 8.8, 4.3 Hz, 4H, Ar–H), 7.48 (dd, J = 8.6, 0.6 Hz, 2H, Ar–H), 7.33 (d, J = 7.9 Hz, 2H, Ar–H), 6.99 (d, J = 9.1 Hz, 2H, Ar–H), 2.43 (s, 3H, CH$_3$), 2.38 (s, 3H, CH$_3$); ^{13}C NMR (75 MHz, DMSO, δ = ppm): 165.39 (C=O), 145.69 (Ar–C), 144.38 (Ar–C), 141.74 (Ar–C), 138.23 (Ar–C), 131.70 (Ar–C), 131.33 (Ar–C), 130.16 (Ar–CH), 128.89 (Ar–CH), 128.23 (Ar–CH), 127.65 (Ar–CH), 122.22 (Ar–CH), 121.28 (Ar–CH), 21.13 (CH$_3$), 20.97 (CH$_3$); HRMS (ESI-TOF) m/z: calcd [M + H]$^+$ for C$_{21}$H$_{19}$NO$_4$S, 382.1113; found, 382.1111.

4.2.2.2. 4-(4-methylbenzamido)phenyl Benzenesulfonate (4b). Yield: 66%; brown solid; mp: 195−196 °C; FT-IR ($\bar{v}$, cm^1, neat): 3358 (N−H, stretching), 1652 (C=O, stretching), 1603, 1528, 1343, 1172, 1143, 1092; ^{1}H NMR (500 MHz, DMSO, δ = ppm): 10.26 (s, 1H, CONH), 7.90−7.80 (m, 5H, Ar–H), 7.75 (d, J = 9.0 Hz, 2H, Ar–H), 7.68 (t, J = 7.8 Hz, 2H, Ar–H), 7.33 (d, J = 8.0 Hz, 2H, Ar–H), 7.00 (d, J = 9.0 Hz, 2H, Ar–H), 2.38 (s, 3H, CH$_3$); ^{13}C NMR (126 MHz, DMSO, δ = ppm): 165.91 (C=O), 144.81 (Ar–C), 142.26 (Ar–C), 138.82 (Ar–C), 135.47 (Ar–C), 134.72 (Ar–C), 132.20 (Ar–C), 130.27 (Ar–CH), 129.41 (Ar–CH), 128.72 (Ar–CH), 128.17 (Ar–CH), 122.74 (Ar–CH), 121.79 (Ar–CH), 21.48 (CH$_3$); HRMS (EI, 70 eV), [C$_{20}$H$_{17}$O$_4$N$_1$S$_1$], 367.08728; found, 367.08709.

4.2.2.3. 4-(4-methylbenzamido)phenyl 4-Iodobenzenesulfonate (4c). Yield: 82%; off-white solid; mp: 223−226 °C; FT-IR ($\bar{v}$, cm^1, neat): 3340 (N−H, stretching), 2921, 2851 (C−H, stretching), 1650 (C=O, stretching), 1522, 1504, 1349, 1195, 1176, 1090; ^{1}H NMR (250 MHz, DMSO, δ = ppm): 10.26 (s, 1H, CONH), 8.04 (d, J = 8.6 Hz, 2H, Ar–H), 7.79 (dd, J = 18.9, 8.7 Hz, 4H, Ar–H), 7.57 (d, J = 8.6 Hz, 2H, Ar–H), 7.31 (d, J = 8.0 Hz, 2H, Ar–H), 7.01 (d, J = 9.1 Hz, 2H, Ar–H), 2.36 (s, 3H, CH$_3$); ^{13}C NMR (63 MHz, DMSO, δ = ppm): 165.46 (C=O), 144.24 (Ar–C), 141.81 (Ar–C), 138.73 (Ar–C), 138.47 (Ar–C), 133.80 (Ar–C), 131.73 (Ar–C), 129.69 (Ar–CH), 128.94 (Ar–CH), 127.71 (Ar–CH), 122.31 (Ar–CH), 121.39 (Ar–CH), 104.10 (Ar–CH), 21.02 (CH$_3$); HRMS (ESI-TOF) m/z: calcd [M + H]$^+$ for C$_{20}$H$_{16}$NO$_4$S$_1$, 493.9923; found, 493.9924.

4.2.2.4. 4-(4-Methylbenzamido)phenyl 4-Methoxybenzenesulfonate (4d). Yield: 61%; light-brown solid; mp: 193−195 °C; FT-IR ($\bar{v}$, cm^1, neat): 3377 (N−H, stretching), 2981 (C−H, stretching), 1660 (C=O, stretching), 1596, 1498, 1362, 1168, 1149, 1094; ^{1}H NMR (250 MHz, DMSO, δ = ppm): 10.26 (s, 1H, CONH), 7.85 (d, J = 8.2 Hz, 2H, Ar–H), 7.76 (dd, J = 9.1, 4.0 Hz, 4H, Ar–H), 7.38−7.28 (m, 2H, Ar–H), 7.17 (d, J = 9.1 Hz, 2H, Ar–H), 6.99 (d, J = 9.1 Hz, 2H, Ar–H), 3.87 (s, 3H, OCH$_3$), 2.38 (s, 3H, CH$_3$); ^{13}C NMR (63 MHz, DMSO, δ = ppm): 165.42 (C=O), 163.97 (Ar–C), 144.47 (Ar–C), 141.77 (Ar–C), 138.22 (Ar–C), 131.75 (Ar–C), 130.65 (Ar–CH), 128.92 (Ar–CH), 127.69 (Ar–CH), 125.45 (Ar–C), 122.32 (Ar–CH), 121.29 (Ar–CH), 114.92 (Ar–CH), 55.91 (OCH$_3$), 21.00 (CH$_3$); HRMS (ESI-TOF) m/z: calcd [M + H]$^+$ for C$_{21}$H$_{19}$NO$_5$S, 398.1062; found, 398.1062.

4.2.2.5. 4-(4-Methylbenzamido)phenyl 4-Chlorobenzenesulfonate (4e). Yield: 77%; brown solid; mp: 196−197 °C; FT-IR ($\bar{v}$, cm^1, neat): 3354 (N−H, stretching), 1652 (C=O, stretching), 1524, 1506, 1376, 1176, 1151, 1090; ^{1}H NMR (250 MHz, DMSO, δ = ppm): 10.28 (s, 1H, CONH), 7.91−7.81 (m, 4H, Ar–H), 7.77 (dd, J = 9.0, 4.7 Hz, 4H, Ar–H), 7.34 (d, J = 7.9 Hz, 2H, Ar–H), 7.04 (d, J = 9.1 Hz, 2H, Ar–H), 2.39 (s, 3H, CH$_3$); ^{13}C NMR (63 MHz, DMSO, δ = ppm): 165.44 (C=O), 144.20 (Ar–C), 141.80 (Ar–C), 140.03 (Ar–C), 138.49 (Ar–C), 133.02 (Ar–C), 131.72 (Ar–C), 130.21 (Ar–CH), 130.00 (Ar–CH), 128.93 (Ar–CH), 127.70 (Ar–CH), 122.31 (Ar–

CH), 121.38 (Ar–CH), 21.00 (CH$_3$); HRMS (ESI-TOF) m/z: calcd [M + H]$^+$ for C$_{20}$H$_{16}$NO$_4$SCl, 402.0567; found, 402.0569.

4.2.2.6. 4-(4-Methylbenzamido)phenyl 4-Propylbenzenesulfonate (4f). Yield: 67%; light-brown solid; mp: 179−180 °C; FT-IR ($\bar{v}$, cm^1, neat): 3369 (N−H, stretching), 2965, 2930, 2860 (C−H, stretching), 1658 (C=O, stretching), 1607, 1524, 1504, 1364, 1174, 1149, 1090; ^{1}H NMR (250 MHz, DMSO, δ = ppm): 10.26 (s, 1H, CONH), 7.85 (d, J = 8.2 Hz, 2H, Ar–H), 7.75 (dd, J = 8.8, 1.8 Hz, 4H, Ar–H), 7.48 (d, J = 8.6 Hz, 2H, Ar–H), 7.36−7.30 (m, 2H, Ar–H), 6.98 (d, J = 9.1 Hz, 2H, Ar–H), 2.74−2.61 (m, 2H, CH$_2$), 2.38 (s, 3H, Ar–CH$_3$), 1.62 (m, 2H, CH$_2$), 0.88 (t, J = 7.3 Hz, 3H, CH$_3$); ^{13}C NMR (63 MHz, DMSO, δ = ppm): 165.41 (C=O), 150.02 (Ar–C), 144.38 (Ar–C), 141.77 (Ar–C), 138.29 (Ar–C), 131.73 (Ar–C), 131.60 (Ar–C), 129.61 (Ar–CH), 128.92 (Ar–CH), 128.31 (Ar–CH), 127.69 (Ar–CH), 122.26 (Ar–CH), 121.26 (Ar–CH), 36.92 (CH$_2$), 23.51 (CH$_2$), 21.00 (CH$_3$), 13.41 (CH$_3$); HRMS (ESI-TOF) m/z: calcd [M + H]$^+$ for C$_{23}$H$_{23}$NO$_4$S, 410.1426; found, 410.1426.

4.2.2.7. 4-(4-Methylbenzamido)phenyl 4-(Trifluoromethoxy)benzenesulfonate (4g). Yield: 71%; colorless solid; mp: 196−198 °C; FT-IR ($\bar{v}$, cm^1, neat): 3348 (N−H, stretching), 1652 (C=O, stretching), 1524, 1508, 1353, 1193, 1141, 1094; ^{1}H NMR (250 MHz, DMSO, δ = ppm): 10.28 (s, 1H, CONH), 8.01 (d, J = 9.1 Hz, 2H, Ar–H), 7.81 (dd, J = 16.5, 8.7 Hz, 4H, Ar–H), 7.66 (dd, J = 9.0, 1.0 Hz, 2H, Ar–H), 7.33 (d, J = 7.9 Hz, 2H, Ar–H), 7.03 (d, J = 9.1 Hz, 2H, Ar–H), 2.38 (s, 3H, CH$_3$); ^{13}C NMR (63 MHz, DMSO, δ = ppm): 165.41 (C=O), 152.45 (Ar–C), 144.12 (Ar–C), 141.76 (Ar–C), 138.50 (Ar–C), 132.90 (Ar–C), 131.67 (Ar–C), 131.12 (Ar–C), 128.88 (CF$_3$), 127.66 (Ar–CH), 122.26 (Ar–CH), 121.78 (Ar–CH), 121.61 (Ar–CH), 121.31 (Ar–CH), 20.95 (CH$_3$); ^{19}F NMR (282 MHz, DMSO) δ −56.73 (s); HRMS (ESI-TOF) m/z: calcd [M + H]$^+$ for C$_{21}$H$_{16}$NO$_5$SF$_3$, 452.0779; found, 452.0780.

4.2.2.8. 4-(4-Methylbenzamido)phenyl [1,1'-Biphenyl]-4-sulfonate (4h). Yield: 71%; colorless solid; mp: 243−244 °C; FT-IR ($\bar{v}$, cm^1, neat): 3360 (N−H, stretching), 1654 (C=O, stretching), 1531, 1508, 1347, 1193, 1174, 1098; ^{1}H NMR (250 MHz, DMSO, δ = ppm): 10.23 (s, 1H, CONH), 7.99−7.86 (m, 4H, Ar–H), 7.81 (d, J = 8.2 Hz, 2H, Ar–H), 7.78−7.69 (m, 4H, Ar–H), 7.52−7.39 (m, 3H, Ar–H), 7.32 (dd, J = 12.7, 7.6 Hz, 2H, Ar–H), 7.07−6.98 (m, 2H, Ar–H), 2.34 (s, 3H, CH$_3$); ^{13}C NMR (63 MHz, DMSO, δ = ppm): 165.43 (C=O), 146.13 (Ar–C), 144.37 (Ar–C), 141.78 (Ar–C), 138.37 (Ar–C), 137.82 (Ar–C), 132.95 (Ar–C), 131.73 (Ar–C), 129.23 (Ar–CH), 129.04 (Ar–CH), 128.93 (Ar–CH), 127.79 (Ar–CH), 127.69 (Ar–CH), 127.24 (Ar–CH), 125.98 (Ar–CH), 122.32 (Ar–CH), 121.37 (Ar–CH), 21.00 (CH$_3$); HRMS (ESI-TOF) m/z: calcd [M + H]$^+$ for C$_{26}$H$_{21}$NO$_4$S, 444.1270; found, 444.1265.

4.2.2.9. 4-(4-Methylbenzamido)phenyl Phenylmethanesulfonate (4i). Yield: 73%; light-brown solid; mp: 205−206 °C; FT-IR ($\bar{v}$, cm^1, neat): 3360 (N−H, stretching), 2940 (C−H, stretching), 1650 (C=O, stretching), 1524, 1506, 1341, 1195, 1143, 1102, 1073; ^{1}H NMR (250 MHz, DMSO, δ = ppm): 10.31 (s, 1H, CONH), 7.86 (dd, J = 8.6, 7.6 Hz, 4H, Ar–H), 7.51 (dd, J = 6.8, 3.2 Hz, 2H, Ar–H), 7.47−7.40 (m, 3H, Ar–H), 7.38−7.31 (m, 2H, Ar–H), 7.22 (d, J = 9.1 Hz, 2H, Ar–H), 4.95 (s, 2H, CH$_2$), 2.39 (s, 3H, CH$_3$); ^{13}C NMR (63 MHz, DMSO, δ = ppm): 165.43 (C=O), 144.40 (Ar–C), 141.78 (Ar–C), 138.15 (Ar–C), 131.77 (Ar–C), 131.07 (Ar–C), 128.94 (CH), 128.81 (CH), 128.65 (CH), 128.11 (C), 127.72

(CH), 122.32 (CH), 121.48 (CH), 55.73 (CH$_2$), 21.01 (CH$_3$); HRMS (ESI-TOF) m/z: calcd [M + H]$^+$ for C$_{21}$H$_{19}$O$_4$NS, 382.1113; found, 382.1116.

4.2.2.10. 4-(4-Methylbenzamido)phenyl 4-Butylbenzenesulfonate (4j). Yield: 80%; colorless solid; mp, 187−188 °C; FT-IR ($\overline{v}$, cm^1, neat): 3371 (N−H, stretching), 2954, 2934, 2858 (C−H, stretching), 1660 (C=O, stretching), 1524, 1504, 1366, 1174, 1149, 1092; ^{1}H NMR (250 MHz, DMSO, δ = ppm): 10.26 (s, 1H, CONH), 7.84 (d, J = 8.2 Hz, 2H, Ar−H), 7.79−7.68 (m, 4H, Ar−H), 7.48 (d, J = 8.5 Hz, 2H, Ar−H), 7.41−7.24 (m, 2H, Ar−H), 6.98 (d, J = 9.2 Hz, 2H, Ar−H), 2.78−2.61 (m, 2H, CH$_2$), 2.38 (s, 3H, CH$_3$), 1.69−1.46 (m, 2H, CH$_2$), 1.28 (m, 2H, CH$_2$), 0.89 (t, J = 7.3 Hz, 3H, CH$_3$); ^{13}C NMR (63 MHz, DMSO, δ = ppm): 165.37 (C=O), 150.23 (Ar−C), 144.34 (Ar−C), 141.73 (Ar−C), 138.25 (Ar−C), 131.69 (Ar−C), 131.51 (Ar−C), 129.51 (Ar−C), 128.88 (Ar−C), 128.28 (Ar−C), 127.65 (Ar−C), 122.22 (Ar−C), 121.21 (Ar−C), 34.59 (CH$_2$), 32.43 (CH$_2$), 21.58 (CH$_2$), 20.96 (CH$_3$), 13.65 (CH$_3$); HRMS (ESI-TOF) m/z: calcd [M + H]$^+$ for C$_{24}$H$_{25}$NO$_4$S, 424.1582; found, 424.1580.

4.2.2.11. 4-(4-Methylbenzamido)phenyl 4-Fluorobenzenesulfonate (4k). Yield: 69%; colorless solid; mp: 185−187 °C; FT-IR ($\overline{v}$, cm^1, neat): 3360 (N−H, stretching), 1652 (C=O, stretching), 1527, 1508, 1491, 1347, 1191, 1172, 1092; ^{1}H NMR (300 MHz, DMSO, δ = ppm): 10.27 (s, 1H, CONH), 7.93 (dd, J = 9.0, 5.0 Hz, 2H, Ar−H), 7.84 (d, J = 8.2 Hz, 2H, Ar−H), 7.77 (d, J = 9.1 Hz, 2H, Ar−H), 7.51 (t, J = 8.9 Hz, 2H, Ar−H), 7.32 (d, J = 7.9 Hz, 2H, Ar−H), 7.01 (d, J = 9.1 Hz, 2H, Ar−H), 2.37 (s, 3H, CH$_3$); ^{13}C NMR (75 MHz, DMSO, δ = ppm): 167.20 (C=O), 165.41, 163.83, 144.22 (Ar−C), 141.75 (Ar−C), 138.41 (Ar−C), 131.86−131.39 (m, Ar−C), 130.47 (d, J = 3.0 Hz, Ar−CH), 128.89 (Ar−CH), 127.66 (Ar−CH), 122.29 (Ar−CH), 121.32 (Ar−CH), 117.12 (d, J = 23.1 Hz, Ar−CH), 20.96 (CH$_3$); ^{19}F NMR (282 MHz, DMSO, δ = ppm): −102.54 (s); HRMS (EI, 70 eV), [C$_{20}$H$_{16}$O$_4$N$_1$F$_1$S$_1$], 385.07786; found, 385.07785.

4.2.2.12. 4-(4-Methylbenzamido)phenyl 2-Fluorobenzenesulfonate (4l). Yield: 71%; off-white solid; mp: 178−181 °C; FT-IR ($\overline{v}$, cm^1, neat): 3354 (N−H, stretching), 1654 (C=O, stretching), 1599, 1524, 1502, 1479, 1353, 1188, 1123, 1075; ^{1}H NMR (250 MHz, DMSO, δ = ppm): 10.26 (s, 1H, CONH), 7.89 (ddd, J = 7.5, 2.5, 1.4 Hz, 1H, Ar−H), 7.86−7.72 (m, 5H, Ar−H), 7.62 (ddd, J = 10.5, 8.4, 1.0 Hz, 1H), 7.47−7.37 (m, 1H, Ar−H), 7.36−7.25 (m, 2H, Ar−H), 7.12−7.01 (m, 2H, Ar−H), 2.36 (s, 3H, CH$_3$); ^{13}C NMR (63 MHz, DMSO, δ = ppm): 165.41 (C=O), 144.05 (Ar−C), 141.76 (Ar−C), 138.56 (Ar−C), 138.14 (d, J = 8.9 Hz, Ar−C), 131.66 (Ar−C), 131.17 (Ar−C), 128.88 (Ar−CH), 127.66 (Ar−CH), 125.49 (d, J = 3.7 Hz, Ar−CH), 122.31−121.04 (m, Ar−CH), 118.02 (Ar−CH), 117.70 (Ar−CH), 20.96 (CH$_3$); ^{19}F NMR (282 MHz, DMSO, δ = ppm): −108.09 (ddd, J = 10.6, 7.1, 5.2 Hz); HRMS (EI, 70 eV), [C$_{20}$H$_{16}$O$_4$N$_1$F$_1$S$_1$], 385.07786; found, 385.07770.

4.2.2.13. 4-Benzamidophenyl 4-Methoxybenzenesulfonate (4m). Yield: 60%; colorless solid; mp: 197−199 °C; FT-IR ($\overline{v}$, cm^1, neat): 3365 (N−H, stretching), 1660 (C=O, stretching), 1524, 1500, 1362, 1261, 1149, 1094; ^{1}H NMR (250 MHz, DMSO, δ = ppm): 10.35 (s, 1H, CONH), 7.93 (dd, J = 8.1, 1.6 Hz, 2H, Ar−H), 7.82−7.71 (m, 4H, Ar−H), 7.63−7.47 (m, 3H, Ar−H), 7.23−7.13 (m, 2H, Ar−H), 7.05−6.95 (m, 2H, Ar−H), 3.88 (s, 3H, OCH$_3$); ^{13}C NMR (63 MHz, DMSO, δ = ppm): 165.59 (C=O), 163.93, 144.51 (Ar−C), 138.10 (Ar−C), 134.62 (Ar−C), 131.67 (Ar−C), 130.62 (Ar−C), 128.37 (Ar−CH), 127.60 (Ar−CH), 125.40 (Ar−CH), 122.31 (Ar−

CH), 121.28 (Ar−CH), 114.89 (Ar−CH), 55.88 (OCH$_3$); HRMS (ESI-TOF) m/z: calcd [M + H]$^+$ for C$_{20}$H$_{17}$NO$_5$S, 384.0905; found, 384.0906.

4.2.2.14. 4-Benzamidophenyl Phenylmethanesulfonate (4n). Yield: 76%; light-yellow solid; mp: 179−181 °C; FT-IR ($\overline{v}$, cm^1, neat): 3288 (N−H, stretching), 2936 (C−H, stretching), 1650 (C=O, stretching), 1524, 1504, 1351, 1184, 1147, 1100, 1073; ^{1}H NMR (300 MHz, DMSO, δ = ppm): 10.40 (s, 1H, CONH), 7.96 (dd, J = 8.2, 1.5 Hz, 2H, Ar−H), 7.86 (d, J = 9.1 Hz, 2H, Ar−H), 7.60 (dd, J = 5.1, 3.5 Hz, 1H, Ar−H), 7.56 (d, J = 7.3 Hz, 2H, Ar−H), 7.51 (dd, J = 5.2, 1.8 Hz, 2H, Ar−H), 7.45 (dd, J = 5.0, 1.8 Hz, 3H, Ar−H), 7.24 (d, J = 9.1 Hz, 2H, Ar−H), 4.96 (s, 2H, CH$_2$); ^{13}C NMR (75 MHz, DMSO, δ = ppm): 165.63 (C=O), 144.48 (Ar−CH), 138.07 (Ar−CH), 134.67 (Ar−C), 131.72 (Ar−C), 131.07 (Ar−C), 128.82 (Ar−CH), 128.65 (Ar−CH), 128.42 (Ar−CH), 128.10 (Ar−CH), 127.67 (Ar−CH), 122.35 (Ar−CH), 121.51 (Ar−CH), 55.73 (CH$_2$); HRMS (ESI-TOF) m/z: calcd [M + H]$^+$ for C$_{20}$H$_{17}$NO$_4$S, 368.0956; found, 368.0955.

4.2.2.15. 4-Benzamidophenyl 4-Propylbenzenesulfonate (4o). Yield: 78%; off-white solid; mp: 192−195 °C; FT-IR ($\overline{v}$, cm^1, neat): 3362 (N−H, stretching), 2957, 2926, 2860 (C−H, stretching), 1656 (C=O, stretching), 1522, 1502, 1407, 1370, 1174, 1151, 1092; ^{1}H NMR (300 MHz, CDCl$_3$, δ = ppm): 10.35 (s, 1H, CONH), 7.96−7.89 (m, 2H, Ar−H), 7.76 (dd, J = 8.8, 2.1 Hz, 4H, Ar−H), 7.64−7.56 (m, 1H, Ar−H), 7.51 (dd, J = 14.2, 7.9 Hz, 4H, Ar−H), 6.99 (d, J = 9.1 Hz, 2H, Ar−H), 2.72−2.59 (m, 2H, CH$_2$), 1.62 (m, 2H, CH$_2$), 0.88 (t, J = 7.3 Hz, 3H, CH$_3$); ^{13}C NMR (75 MHz, DMSO, δ = ppm): 165.60 (C=O), 150.01 (Ar−C), 144.44 (Ar−C), 138.18 (Ar−C), 134.62 (Ar−C), 131.68 (Ar−C), 131.57 (Ar−C), 129.59 (Ar−CH), 128.38 (Ar−CH), 128.28 (Ar−CH), 127.62 (Ar−CH), 122.27 (Ar−CH), 121.27 (Ar−CH), 36.90 (CH$_2$), 23.49 (CH$_2$), 13.39 (CH$_3$); HRMS (ESI-TOF) m/z: calcd [M + H]$^+$ for C$_{22}$H$_{21}$NO$_4$S, 396.1270; found, 396.1271.

4.2.2.16. 4-Benzamidophenyl [1,1′-Biphenyl]-4-sulfonate (4p). Yield: 66%; off-white solid; mp: 220−222 °C; FT-IR ($\overline{v}$, cm^1, neat): 3367 (N−H, stretching), 1658 (C=O, stretching), 1605, 1524, 1502, 1405, 1347, 1312, 1193, 1143, 1098; ^{1}H NMR (300 MHz, DMSO, δ = ppm): 10.36 (s, 1H, CONH), 7.98 (d, J = 8.8 Hz, 2H, Ar−H), 7.92 (m, 4H, Ar−H), 7.80 (d, J = 2.0 Hz, 2H, Ar−H), 7.77 (m, 2H, Ar−H), 7.56 (m, 3H, Ar−H), 7.50 (m, 3H, Ar−H), 7.07 (d, J = 9.1 Hz, 2H, Ar−H); ^{13}C NMR (75 MHz, DMSO, δ = ppm): 165.65 (C=O), 146.14 (Ar−C), 144.45 (Ar−C), 138.29 (Ar−C), 137.82 (Ar−C), 134.65 (Ar−C), 132.95 (Ar−C), 131.71 (Ar−C), 129.23 (Ar−CH), 129.03 (Ar−CH), 128.93 (Ar−CH), 128.40 (Ar−CH), 127.80 (Ar−CH), 127.65 (Ar−CH), 127.23 (Ar−CH), 122.35 (Ar−CH), 121.40 (Ar−CH); HRMS (ESI-TOF) m/z: calcd [M + H]$^+$ for C$_{25}$H$_{19}$NO$_4$S, 430.1113; found, 430.1113.

4.2.2.17. 4-Benzamidophenyl Quinoline-8-sulfonate (4q). Yield: 69%; yellowish-white solid; mp: 173−175 °C; FT-IR ($\overline{v}$, cm^1, neat): 3329 (N−H, stretching), 1646 (C=O, stretching), 1607, 1524, 1504, 1366, 1316, 1174, 1158, 1075; ^{1}H NMR (300 MHz, DMSO, δ = ppm): 10.29 (s, 1H, CONH), 9.25 (dd, J = 4.2, 1.8 Hz, 1H, Ar−NH), 8.63 (dd, J = 8.4, 1.7 Hz, 1H, Ar−H), 8.45 (dd, J = 8.2, 1.4 Hz, 1H, Ar−H), 8.35 (dd, J = 7.4, 1.4 Hz, 1H, Ar−H), 7.88 (m, 2H, Ar−H), 7.79 (m, 2H, Ar−H), 7.66 (d, J = 9.1 Hz, 2H, Ar−H), 7.56 (d, J = 7.1 Hz, 1H, Ar−H), 7.50 (dd, J = 8.0, 6.4 Hz, 2H, Ar−H), 6.96 (d, J = 9.1 Hz, 2H, Ar−H); ^{13}C NMR (75 MHz, DMSO, δ = ppm): 165.57 (C=O), 152.43, 144.77, 143.11, 137.99 (Ar−C), 137.15 (Ar−C), 136.24 (Ar−C), 134.64 (Ar−C), 134.01, 131.66, 131.36, 128.76 (Ar−CH),

128.37 (Ar−CH), 127.61 (Ar−CH), 125.64 (Ar−CH), 123.07 (Ar−CH), 122.05 (Ar−CH), 121.37 (Ar−CH); HRMS (ESI-TOF) m/z: calcd [M + H]$^+$ for $C_{22}H_{16}N_2O_4S$, 405.0909; found, 405.0914.

4.2.2.18. 4-Benzamidophenyl 4-Iodobenzenesulfonate (4r). Yield: 62%; off-white solid; mp: 211−216 °C; FT-IR ($\overline{v}$, cm^1, neat): 3365 (N−H, stretching), 1660 (C=O, stretching), 1520, 1502, 1368, 1172, 1149, 1085; ^{1}H NMR (300 MHz, CDCl$_3$, δ = ppm): 10.37 (s, 1H, CONH), 8.07 (d, J = 8.6 Hz, 2H, Ar−H), 7.97−7.89 (m, 2H, Ar−H), 7.78 (d, J = 9.1 Hz, 2H, Ar−H), 7.60 (d, J = 8.6 Hz, 3H, Ar−H), 7.53 (dd, J = 8.0, 6.3 Hz, 2H, Ar−H), 7.04 (d, J = 9.1 Hz, 2H, Ar−H); ^{13}C NMR (75 MHz, CDCl$_3$, δ = ppm): 165.64 (C=O), 144.28 (Ar−C), 138.70 (Ar−CH), 138.36, 134.62, 133.77, 131.70 (Ar−C), 129.65 (Ar−CH), 128.39 (Ar−CH), 127.63 (Ar−CH), 122.30 (Ar−CH), 121.39 (Ar−CH), 104.08 (Ar−C); HRMS (ESI-TOF) m/z: calcd [M + H]$^+$ for $C_{19}H_{14}NO_4SI$, 479.9766; found, 479.9761.

4.2.2.19. 4-Benzamidophenyl 4-Fluorobenzenesulfonate (4s). Yield: 73%; light-brown solid; mp: 190−192 °C; FT-IR ($\overline{v}$, cm^1, neat): 3373 (N−H, stretching), 1658 (C=O, stretching), 1590, 1524, 1491, 1407, 1378, 1242, 1176, 1151, 1090; ^{1}H NMR (500 MHz, DMSO, δ = ppm): 10.37 (s, 1H, CONH), 7.94 (dd, J = 12.0, 6.2 Hz, 4H, Ar−H), 7.78 (d, J = 9.0 Hz, 2H, Ar−H), 7.59 (d, J = 7.3 Hz, 1H, Ar−H), 7.52 (m, 4H, Ar−H), 7.03 (d, J = 9.0 Hz, 2H, Ar−H); ^{13}C NMR (126 MHz, DMSO, δ = ppm): 166.58 (C=O), 165.67 (Ar−C), 164.55 (Ar−C), 144.34 (Ar−C), 138.38 (Ar−C), 134.65 (Ar−C), 131.85−131.46 (m), 130.49, 128.42 (Ar−CH), 127.66 (Ar−CH), 122.37 (Ar−CH), 121.39 (Ar−CH), 117.18 (d, J = 23.1 Hz, Ar−CH); ^{19}F NMR (471 MHz, DMSO, δ = ppm): −102.52 (s); HRMS (EI, 70 eV), [$C_{19}H_{14}O_4N_1F_1S_1$], 371.06221; found, 371.06190.

4.2.2.20. 4-Benzamidophenyl 4-(trifluoromethoxy)-benzenesulfonate (4t). Yield: 78%; off-white solid; mp: 184−186 °C; FT-IR ($\overline{v}$, cm^1, neat): 3365 (N−H, stretching), 1658 (C=O, stretching), 1607, 1526, 1407, 1382, 1151, 1090; ^{1}H NMR (300 MHz, DMSO, δ = ppm): 10.38 (s, 1H, CONH), 8.03 (d, J = 8.9 Hz, 2H, Ar−H), 7.93 (m, 2H, Ar−H), 7.79 (d, J = 9.1 Hz, 2H, Ar−H), 7.67 (dd, J = 8.9, 1.0 Hz, 2H, Ar−H), 7.60 (d, J = 7.0 Hz, 1H, Ar−H), 7.54 (m, 2H, Ar−H), 7.06 (d, J = 9.1 Hz, 2H, Ar−H); ^{13}C NMR (75 MHz, DMSO, δ = ppm): 165.67 (C=O), 152.49 (Ar−C), 144.24 (Ar−C), 138.46 (Ar−C), 134.63, 132.94 (Ar−C), 131.73 (Ar−CH), 131.16 (CF$_3$), 128.41 (Ar−CH), 127.66 (Ar−CH), 122.34 (Ar−CH), 121.68 (Ar−CH), 121.38 (Ar−CH); ^{19}F NMR (282 MHz, DMSO, δ = ppm): −56.73 (s); HRMS (ESI-TOF) m/z: calcd [M + H]$^+$ for $C_{20}H_{14}F_3NO_5S$; 438.0623; found, 438.0616.

4.2.3. Synthesis of N-(4-Hydroxyphenyl)-9-methyl-9H-fluorene-9-carboxamide (6). Compound **6** was synthesized by the reaction of 4-aminophenol (**1**) (4.12 mmol; 0.450 g) with 9-methyl-9*H*-fluorene-9-carbonyl chloride (**5**) (2.50 mmol; 0.605 g) in acetone (50 mL) and base anhydrous potassium carbonate (3.62 mmol; 0.500 g). The reaction proceeded as per conditions followed for the synthesis of **3a** and **3b**.

4.2.4. Synthesis of Arylamide Sulphonates 7a−F. The desired sulphonate derivatives **7a−f** were produced by the reaction of N-(4-hydroxyphenyl)-9-methyl-9H-fluorene-9-carboxamide (**6**) (0.485 mmol; 0.152 g) with alkyl or aryl sulfonyl chloride derivatives (0.980 mmol) in dry tetrahydrofuran (THF) (12 mL). Triethylamine (2.10 mmol) was added dropwise to the stirring mixture at 0 °C. The reaction proceeded as per the protocol used for the synthesis of compounds **4a−l** and **4m−t**.

4.2.4.1. 4-(9-Methyl-9H-fluorene-9-carboxamido)phenyl 2-Fluorobenzenesulfonate (7a). Yield: 77%; dark-brown solid; mp: 146−147 °C; FT-IR ($\overline{v}$, cm^1, neat): 3053 (N−H, stretching), 2833 (C−H, stretching), 1691 (C=O, stretching), 1479, 1460, 1413, 1221, 1092; ^{1}H NMR (300 MHz, CDCl$_3$, δ = ppm): 7.75−7.68 (m, 2H, Ar−H), 7.64−7.48 (m, 4H, Ar−H), 7.37 (td, J = 7.5, 1.3 Hz, 2H, Ar−H), 7.29 (td, J = 7.4, 1.3 Hz, 2H, Ar−H), 7.19−7.06 (m, 4H, Ar−H), 6.83 (d, J = 9.0 Hz, 2H, Ar−H), 6.63 (s, 1H, CONH), 1.73 (s, 3H, CH$_3$); ^{13}C NMR (75 MHz, CDCl$_3$, δ = ppm): 171.63 (C=O), 161.13, 157.69, 147.21, 145.23, 140.33, 136.87 (d, J = 8.1 Hz), 131.58, 128.85, 128.46, 124.62 (d, J = 4.0 Hz), 124.18, 123.41 (d, J = 13.7 Hz), 122.47, 120.84 (d, J = 5.3 Hz), 117.46 (d, J = 20.7 Hz), 59.04, 23.07 (CH$_3$); HRMS (ESI-TOF) m/z: calcd [M + H]$^+$ for $C_{27}H_{20}FNO_4S$, 474.1175; found; 474.1178.

4.2.4.2. 4-(9-Methyl-9H-fluorene-9-carboxamido)phenyl Trifluoromethanesulfonate (7b). Yield: 68%; off-white solid; mp: 140−141 °C; FT-IR ($\overline{v}$, cm^1, neat): 3290 (N−H, stretching), 2965, 2928 (C−H, stretching), 1667 (C=O, stretching), 1508, 1419, 1207, 1133, 1013; ^{1}H NMR (500 MHz, CDCl$_3$, δ = ppm): 7.82 (d, J = 7.6 Hz, 2H, Ar−H), 7.63 (d, J = 7.5 Hz, 2H, Ar−H), 7.48 (td, J = 7.5, 0.9 Hz, 2H, Ar−H), 7.40 (td, J = 7.5, 0.9 Hz, 2H, Ar−H), 7.34 (d, J = 9.1 Hz, 2H, Ar−H), 7.09 (d, J = 9.1 Hz, 2H, Ar−H), 6.76 (s, 1H, CONH), 2.17 (s, 3H, CH$_3$); ^{13}C NMR (126 MHz, CDCl$_3$, δ = ppm): 171.84 (C=O), 147.19, 145.35, 140.40, 137.79, 128.96, 128.57, 124.24, 121.89, 121.18, 120.89, 59.14, 23.04 (CH$_3$); HRMS (EI, 70 eV), [$C_{22}H_{16}O_4N_1F_3S_1$], 447.07466; found 447.07454.

4.2.4.3. 4-(9-Methyl-9H-fluorene-9-carboxamido)phenyl 4-Fluorobenzenesulfonate (7c). Yield: 79%; colorless solid; mp: 200−201 °C; FT-IR ($\overline{v}$, cm^1, neat): 3303 (N−H, stretching), 3060 (C−H, stretching), 1669 (C=O, stretching), 1491, 1405, 1347, 1240, 1193, 1151, 1092; ^{1}H NMR (500 MHz, CDCl$_3$, δ = ppm): 7.81 (d, J = 7.6 Hz, 2H, Ar−H), 7.76 (dd, J = 8.9, 5.0 Hz, 2H, Ar−H), 7.62 (d, J = 7.5 Hz, 2H, Ar−H), 7.47 (td, J = 7.5, 0.9 Hz, 2H, Ar−H), 7.39 (td, J = 7.5, 0.9 Hz, 2H, Ar−H), 7.22−7.11 (m, 4H, Ar−H), 6.83−6.75 (m, 2H, Ar−H), 6.72 (s, 1H, CONH), 1.83 (s, 3H, CH$_3$); ^{13}C NMR (126 MHz, CDCl$_3$, δ = ppm): 171.65 (C=O), 167.12, 165.07, 147.25, 145.38, 140.36, 136.79, 131.51 (d, J = 9.5 Hz), 131.21 (d, J = 2.9 Hz), 128.87, 128.49, 124.21, 122.79, 120.83, 116.66 (d, J = 22.9 Hz), 59.08, 23.09 (CH$_3$); HRMS (EI, 70 eV), [$C_{27}H_{20}O_4N_1F_1S_1$], 473.10916; found 473.10858.

4.2.4.4. 4-(9-Methyl-9H-fluorene-9-carboxamido)phenyl Methanesulfonate (7d). Yield: 55%; off-white solid; mp: 124−125 °C; FT-IR ($\overline{v}$, cm^1, neat): 3369 (N−H, stretching), 3008, 2926 (C−H, stretching), 1679 (C=O, stretching), 1603, 1504, 1360, 1149; ^{1}H NMR (300 MHz, CDCl$_3$, δ = ppm): 8.28 (ddd, J = 7.6, 1.2, 0.7 Hz, 2H, Ar−H), 8.08 (ddd, J = 7.4, 1.2, 0.7 Hz, 2H, Ar−H), 7.92 (td, J = 7.5, 1.3 Hz, 2H, Ar−H), 7.84 (td, J = 7.4, 1.3 Hz, 2H, Ar−H), 7.73 (d, J = 9.1 Hz, 2H, Ar−H), 7.53 (d, J = 9.1 Hz, 2H, Ar−H), 7.26 (s, 1H, CONH), 3.47 (s, 3H, CH$_3$), 2.29 (s, 3H, CH$_3$); ^{13}C NMR (75 MHz, CDCl$_3$, δ = ppm): 171.58 (C=O), 147.11, 145.03, 140.22, 136.72, 128.74, 128.35, 124.03, 122.33, 121.14, 120.73, 58.89, 37.03 (CH$_3$), 23.01 (CH$_3$); HRMS (EI, 70 eV), [$C_{22}H_{19}O_4N_1S_1$], 393.10293; found 393.10295.

4.2.4.5. 4-(9-Methyl-9H-fluorene-9-carboxamido)phenyl 4-Methylbenzenesulfonate (7e). Yield: 81%; yellowish solid; mp: 145−147 °C; FT-IR ($\overline{v}$, cm^1, neat): 3311 (N−H, stretching), 2973, 2928 (C−H, stretching), 1671 (C=O, stretching), 1502, 1405, 1345, 1195, 1153, 1092; ^{1}H NMR (300 MHz, CDCl$_3$, δ = ppm): 7.80 (ddd, J = 7.6, 1.2, 0.7 Hz, 2H,

Ar—H), 7.65—7.58 (m, 4H, Ar—H), 7.46 (td, J = 7.5, 1.3 Hz, 2H, Ar—H), 7.38 (td, J = 7.5, 1.3 Hz, 2H, Ar—H), 7.26 (d, J = 0.6 Hz, 1H. Ar—H), 7.23 (d, J = 0.7 Hz, 1H, Ar—H), 7.19—7.11 (m, 2H, Ar—H), 6.84—6.74 (m, 2H, Ar—H), 6.70 (s, 1H, CONH), 2.41 (s, 3H, Ar—CH$_3$), 1.82 (s, 3H, CH$_3$); ^{13}C NMR (75 MHz, CDCl$_3$, δ = ppm): 171.60 (C=O), 147.29, 145.62, 145.47, 140.36, 136.56, 132.25, 129.86, 128.85, 128.65, 128.47, 124.22, 122.88, 120.82, 120.72, 59.08, 23.11 (CH$_3$), 21.81(CH$_3$); HRMS (EI, 70 eV), [C$_{28}$H$_{23}$O$_4$N$_1$S$_1$], 469.13423; found 469.13413.

4.2.4.6. 4-(9-Methyl-9H-fluorene-9-carboxamido)phenyl Benzenesulfonate (7f). Yield: 85%; off-white solid; mp: 193—196 °C; FT-IR ($\overline{v}$, cm^1, neat): 3301 (N—H, stretching), 3062 (C—H, stretching), 1669 (C=O, stretching), 1500, 1446, 1405, 1347, 1195, 1153, 1090; ^{1}H NMR (250 MHz, CDCl$_3$, δ = ppm): 7.86—7.70 (m, 4H, Ar—H), 7.67—7.58 (m, 3H, Ar—H), 7.47 (ddd, J = 8.9, 4.9, 1.2 Hz, 4H, Ar—H), 7.38 (td, J = 7.4, 1.3 Hz, 2H, Ar—H), 7.22—7.12 (m, 2H, Ar—H), 6.84—6.75 (m, 2H, Ar—H), 6.72 (s, 1H, CONH), 1.83 (s, 3H, CH$_3$); ^{13}C NMR (63 MHz, CDCl$_3$, δ = ppm): 171.60 (C=O), 147.24, 145.50, 140.34, 136.64, 135.24, 134.31, 129.22, 128.84, 128.59, 128.46, 124.19, 122.81, 120.81, 120.74, 59.06, 23.09 (CH$_3$); HRMS (EI, 70 eV), [C$_{27}$H$_{21}$O$_4$N$_1$S$_1$], 455.11858; , found 455.11860

4.3. Biological Evaluation. *4.3.1. ENPP1 and ENPP3 Transfection.* Transfection was done in COS-7 cells using plasmids expressing human ENPP1 (GenBank accession no. NM_006208) or ENPP3 (GenBank accession no. NM_005021) and "Lipofectamine" as transfection reagent.[38,39] In a 10 cm culture dish plate, COS-7 cells (70—80% confluent cells) were incubated with DMEM/F-12 (lacking FBS) including plasmid DNA (6 μg) and 24 μL of Lipofectamine reagent and incubated for 5 h at 37 °C; then an equal volume of DMEM/F-12 supplemented with 20% FBS was added to stop the process of transfection. The transfected cells were isolated from the media after 48—72 h.[40]

4.3.2. Preparation of Protein Aliquots. The transfected cells were washed with cold Tris-saline buffer (4 °C) and collected in the presence of a harvesting buffer that was composed of 95 mM NaCl and 0.1 mM phenylmethylsulfonyl fluoride (PMSF), 45 mM Trisbase, pH 7.5. The scrapped cells were subjected to washing through centrifugation twice at 300g for 5 min at 4 °C.[30] The cells were sonicated after re-suspension in the harvesting buffer with aprotinin (10 μg/mL) and centrifuged at 850g at 4 °C for 5 min. The supernatant was collected, and aliquots were preserved at −80 °C after adding glycerol (7.5%). For estimation of protein, Bradford microplate assay was applied using bovine serum albumin as ref 41.

4.3.3. Enzyme Inhibition Assay. The effect of synthesized molecules on the activity of isozymes ENPP1 and ENPP3 was evaluated by using the previously reported method with minor changes.[22,38] Initial screening of the compounds was performed at 100 μM concentration per well in triplicate in the buffer: 5 mM MgCl$_2$, 0.1 mM ZnCl$_2$, and 50 mM Tris—HCl, adjusted to pH 9.5—9.6. Briefly, 30 ng ENPP1 and 32 ng ENPP3 proteins per well were added followed by the addition of 100 μM synthesized compounds dissolved in 10% dimethyl sulfoxide (DMSO). The reaction was initiated by adding a substrate (thymidine 5′-monophosphate para-nitrophenyl ester) 300 μM per well and allowed to incubate for 35 min at 37 °C. The reading was taken with the help of a microplate reader (BioTek FLx800, Instruments, Inc., USA) at a wavelength of 405 nm. The compounds presenting more than 50% inhibition of either isozyme were subjected to serial dilutions, and the IC$_{50}$ values

were calculated through the non-linear regression analysis curve fitting program PRISM 5.0 (GraphPad, San Diego, CA, USA).

4.3.4. Enzyme Kinetic Study. The enzyme kinetic study was performed by using a serial concentration of substrate 0, 1.25, 2.5, 5.0, 7.5, and 10 mM. The compound concentrations for **4j** were 0.0, 0.5, 1.0, and 1.5 μM, and for inhibitor **4e,** the used concentrations were 0.0, 0.3, 0.6, and 1.2 μM. The assay plate was prepared by adding the concentrations of enzymes (ENPP1 = 30 ng, ENPP3 = 32 ng) per well to the assay buffer. After adding the serial concentrations of compounds and substrates, the assay mixture was incubated at 37 °C, and the reading was noted for up to 35 min with 5 min intervals by using a microplate reader (BioTek FLx800, Instruments, Inc., USA). The data were analyzed by PRISM 5.0 (Graph Pad, San Diego, CA, USA), and Lineweaver—Burk graphs were plotted.

4.3.5. Cytotoxicity Assay (MTT Assay). The MTT [3-(4,5-dimethylthiazol-2-yl)-2,5-diphenyltetrazolium bromide] assay was applied to check the cytotoxic effect of the compounds with minor modifications in the already reported method.[42] The cells were seeded in 96-well plates at a quantity of about 4×10^4 cells per well and incubated for 24 h in a CO$_2$ incubator. After incubation for 24 h, serum-free media were added to replace the existing media of cell culture, and the cells were treated with test compounds along with positive control at 100 μM concentrations per well. Afterward, the incubation was given for the next 24 h; MTT reagent (0.5 mg/mL) was added and further incubated at 37 °C for 4 h. Dimethylsulfoxide was added to solubilize the violet crystals and a stopping reagent composed of isopropanol (50%) and sodium dodecyl sulfate (10%) was added. The absorbance was measured at 570 nm with the help of a microplate reader (FLUOstar Omega Microplate Reader, Germany), and results were compiled.

4.3.6. Molecular Docking Analysis. For the in silico observations, the available ligand-bounded human crystallographic structures of ENPP1 (PDB ID = 6wew) and ENPP3 (PDB ID = 6C02) were downloaded from PDB.[37,43] The minimization of energy and molecule database of the docked molecules was generated with the help of the Molecular Operating Environment.[44] The protein preparation such as energy minimization, selection of pocket site, removal of water molecules, protonation, and docking studies was performed by using the default system of LeadIT (BioSolveIT GmbH, Germany).[45] Among the selected number of poses for each compound, poses that possessed low binding energy and considerable affinity with the amino acids residues were selected for further visualization by using Discovery Studio Visualizer DS.[46]

■ ASSOCIATED CONTENT

ⓈI Supporting Information

The Supporting Information is available free of charge at https://pubs.acs.org/doi/10.1021/acsomega.2c03473.

> ^{1}H NMR and ^{13}C NMR spectra for compounds and purity analysis through HPLC (PDF)

■ AUTHOR INFORMATION

Corresponding Author

> **Jamshed Iqbal** − *Centre for Advanced Drug Research, COMSATS University Islamabad, Abbottabad 22060, Pakistan; Department of Pharmacy, COMSATS University Islamabad, Abbottabad 22060, Pakistan;* ● orcid.org/0000-

0002-8971-133X; Phone: +92-992-383591-96;
Email: drjamshed@cuiatd.edu.pk; Fax: +92-992-383441

Authors

Saif Ullah − *Centre for Advanced Drug Research, COMSATS University Islamabad, Abbottabad 22060, Pakistan; Department of Pharmacy, COMSATS University Islamabad, Abbottabad 22060, Pakistan*

Julie Pelletier − *Centre de Recherche Du CHU de Québec−Université Laval, Québec G1V 4G2, Canada*

Jean Sévigny − *Centre de Recherche Du CHU de Québec−Université Laval, Québec G1V 4G2, Canada; Département de Microbiologie-infectiologie et D'immunologie, Faculté de Médecine, Université Laval, Québec G1V 0A6, Canada*

Complete contact information is available at:
https://pubs.acs.org/10.1021/acsomega.2c03473

Notes
The authors declare no competing financial interest.

ABBREVIATIONS USED

ENPP	ectonucleotide pyrophosphatase/phosphodiesterase
ATP	adenosine triphosphate
DMSO	dimethyl sulfoxide
MTT reagent	3-(4,5-dimethylthiazol-2-yl)-2,5-diphenyltetrazolium bromide
HEK	human embryonic kidney cell line
HRMS	high-resolution mass spectrometry
DMEM	Dulbecco's modified Eagle's medium
FBS	fetal bovine serum
BSA	bovine serum albumin

REFERENCES

(1) Eliahu, S.; Lecka, J.; Reiser, G.; Haas, M.; Bigonnesse, F.; Lévesque, S. A.; Pelletier, J.; Sévigny, J.; Fischer, B. Diadenosine 5′, 5″-(boranated) polyphosphonate analogues as selective nucleotide pyrophosphatase/phosphodiesterase inhibitors. *J. Med. Chem.* **2010**, *53*, 8485−8497.

(2) Stefan, C.; Jansen, S.; Bollen, M. Modulation of purinergic signaling by NPP-type ectophosphodiesterases. *Purinergic Signalling* **2006**, *2*, 361−370.

(3) Cimpean, A.; Stefan, C.; Gijsbers, R.; Stalmans, W.; Bollen, M. Substrate-specifying determinants of the nucleotide pyrophosphatases/phosphodiesterases NPP1 and NPP2. *Biochem. J.* **2004**, *381*, 71−77.

(4) Aoki, J. Mechanisms of lysophosphatidic acid production. *Cell Dev. Biol.* **2004**, *15*, 477−489.

(5) Aoki, J.; Inoue, A.; Okudaira, S. Two pathways for lysophosphatidic acid production. *Biochim. Biophys. Acta, Mol. Cell Biol. Lipids* **2008**, *1781*, 513−518.

(6) Kawaguchi, M.; Okabe, T.; Okudaira, S.; Hanaoka, K.; Fujikawa, Y.; Terai, T.; Komatsu, T.; Kojima, H.; Aoki, J.; Nagano, T. Fluorescence probe for lysophospholipase C/NPP6 activity and a potent NPP6 inhibitor. *J. Am. Chem. Soc.* **2011**, *133*, 12021−12030.

(7) Sakagami, H.; Aoki, J.; Natori, Y.; Nishikawa, K.; Kakehi, Y.; Natori, Y.; Arai, H. Biochemical and molecular characterization of a novel choline-specific glycerophosphodiester phosphodiesterase belonging to the nucleotide pyrophosphatase/phosphodiesterase family. *J. Biol. Com.* **2005**, *280*, 23084−23093.

(8) Duan, R. D. Alkaline sphingomyelinase: an old enzyme with novel implications. *Biochim. Biophys. Acta Mol. Cell Biol. Lipids* **2006**, *1761*, 281−291.

(9) Takahashi, T.; Old, L. J.; Boyse, E. A. Surface alloantigens of plasma cells. *J. Exp. Med.* **1970**, *131*, 1325−1341.

(10) Rosenthal, A. K.; Hempel, D.; Kurup, I. V.; Masuda, I.; Ryan, L. M. Purine receptors modulate chondrocyte extracellular inorganic pyrophosphate production. *Osteoarthir. Cartil.* **2010**, *18*, 1496−1501.

(11) Zimmermann, H.; Zebisch, M.; Sträter, N. Cellular function and molecular structure of ecto-nucleotidases. *Purinergic Signalling* **2012**, *8*, 437−502.

(12) Zalatan, J. G.; Fenn, T. D.; Brunger, A. T.; Herschlag, D. Structural and functional comparisons of nucleotide pyrophosphatase/phosphodiesterase and alkaline phosphatase: implications for mechanism and evolution. *Biochemistry* **2006**, *45*, 9788−9803.

(13) Kato, K.; Nishimasu, H.; Okudaira, S.; Mihara, E.; Ishitani, R.; Takagi, J.; Aoki, J.; Nureki, O. Crystal structure of Enpp1, an extracellular glycoprotein involved in bone mineralization and insulin signaling. *Proc. Natl. Acad. Sci. U.S.A.* **2012**, *109*, 16876−16881.

(14) Nadel, Y.; Lecka, J.; Gilad, Y.; Ben-David, G.; Förster, D.; Reiser, G.; Kenigsberg, S.; Camden, J.; Weisman, G. A.; Senderowitz, H.; Sévigny, J.; Fischer, B. Highly potent and selective ectonucleotide pyrophosphatase/phosphodiesterase I inhibitors based on an adenosine 5′-(α or γ)-thio-(α, β-or β, γ)-methylenetriphosphate scaffold. *J. Med. Chem.* **2014**, *57*, 4677−4691.

(15) Hausmann, J.; Kamtekar, S.; Christodoulou, E.; Day, J. E.; Wu, T.; Fulkerson, Z.; Albers, H. M.; van Meeteren, L. A.; Houben, A. J.; van Zeijl, L.; Jansen, S.; Andries, M.; Hall, T.; Pegg, L. E.; Benson, T. E.; Kasiem, M.; Harlos, K.; Kooi, C. W. V.; Smyth, S. S.; Ovaa, H.; Bollen, M.; Morris, A. J.; Moolenaar, W. H.; Perrakis, A. Structural basis of substrate discrimination and integrin binding by autotaxin. *Nat. Struct. Mol. Biol.* **2011**, *18*, 198−204.

(16) Addison, W. N.; Azari, F.; Sørensen, E. S.; Kaartinen, M. T.; McKee, M. D. Pyrophosphate inhibits mineralization of osteoblast cultures by binding to mineral, up-regulating osteopontin, and inhibiting alkaline phosphatase activity. *J. Biol. Chem.* **2007**, *282*, 15872−15883.

(17) Bühring, H.-J.; Streble, A.; Valent, P. The basophil-specific ectoenzyme E-NPP3 (CD203c) as a marker for cell activation and allergy diagnosis. *Int. Arch. Allergy Immunol.* **2004**, *133*, 317−329.

(18) Gijsbers, R.; Ceulemans, H.; Stalmans, W.; Bollen, M. Structural and catalytic similarities between nucleotide pyrophosphatases/phosphodiesterases and alkaline phosphatases. *J. Biol. Chem.* **2001**, *276*, 1361−1368.

(19) Scott, L. J.; Delautier, D.; Meerson, N. R.; Trugnan, G.; Goding, J. W.; Maurice, M. Biochemical and molecular identification of distinct forms of alkaline phosphodiesterase I expressed on the apical and basolateral plasma membrane surfaces of rat hepatocytes. *J. Hepatol.* **1997**, *25*, 995−1002.

(20) Villa-Bellosta, R.; Wang, X.; Millán, J. L.; Dubyak, G. R.; O'Neill, W. C. Extracellular pyrophosphate metabolism and calcification in vascular smooth muscle. *Am. J. Physiol. Heart Circ. Physiol.* **2011**, *301*, H61−H68.

(21) Iqbal, J.; Lévesque, S. A.; Sévigny, J.; Müller, C. E. A highly sensitive CE-UV method with dynamic coating of silica-fused capillaries for monitoring of nucleotide pyrophosphatase/phosphodiesterase reactions. *Electrophoresis* **2008**, *29*, 3685−3693.

(22) Ullah, S.; El-Gamal, M. I.; El-Gamal, R.; Pelletier, J.; Sévigny, J.; Shehata, M. K.; Anbar, H. S.; Iqbal, J. Synthesis, biological evaluation, and docking studies of novel pyrrolo [2, 3-b] pyridine derivatives as

both ectonucleotide pyrophosphatase/phosphodiesterase inhibitors and antiproliferative agents. *Eur. J. Med. Chem.* **2021**, *217*, 113339.

(23) Kanwal, A.; Ullah, S.; Ahmad, M.; Pelletier, J.; Aslam, S.; Sultan, S.; Sévigny, J.; Iqbal, M.; Iqbal, J. Synthesis and Nucleotide Pyrophosphatase/Phosphodiesterase Inhibition Studies of Carbohydrazides Based on Benzimidazole-Benzothiazine Skeleton. *ChemistrySelect* **2020**, *5*, 14399−14407.

(24) El-Gamal, M. I.; Ullah, S.; Zaraei, S. O.; Jalil, S.; Zaib, S.; Zaher, D. M.; Omar, H. A.; Anbar, H. S.; Pelletier, J.; Sévigny, J.; Iqbal, J. Synthesis, biological evaluation, and docking studies of new raloxifene sulfonate or sulfamate derivatives as inhibitors of nucleotide pyrophosphatase/phosphodiesterase. *Eur. J. Med. Chem.* **2019**, *181*, 111560.

(25) Anbar, H. S.; El-Gamal, R.; Ullah, S.; Zaraei, S. O.; al-Rashida, M.; Zaib, S.; Pelletier, J.; Sévigny, J.; Iqbal, J.; El-Gamal, M. I. Evaluation of sulfonate and sulfamate derivatives possessing benzofuran or benzothiophene nucleus as inhibitors of nucleotide pyrophosphatases/phosphodiesterases and anticancer agents. *Bioorg. Chem.* **2020**, *104*, 104305.

(26) Semreen, M. H.; El-Gamal, M. I.; Ullah, S.; Jalil, S.; Zaib, S.; Anbar, H. S.; Lecka, J.; Sévigny, J.; Iqbal, J. Synthesis, biological evaluation, and molecular docking study of sulfonate derivatives as nucleotide pyrophosphatase/phosphodiesterase (NPP) inhibitors. *Bioorg. Med. Chem.* **2019**, *27*, 2741−2752.

(27) Shah, P.; Dhameliya, T. M.; Bansal, R.; Nautiyal, M.; Kommi, D. N.; Jadhavar, P. S.; Sridevi, J. P.; Yogeeswari, P.; Sriram, D.; Chakraborti, A. K. N-Arylalkylbenzo [d] thiazole-2-carboxamides as anti-mycobacterial agents: design, new methods of synthesis and biological evaluation. *MedChemComm* **2014**, *5*, 1489−1495.

(28) Tanwar, B.; Kumar, A.; Yogeeswari, P.; Sriram, D.; Chakraborti, A. K. Design, development of new synthetic methodology, and biological evaluation of substituted quinolines as new anti-tubercular leads. *Bioorg. Med. Chem. Lett.* **2016**, *26*, 5960−5966.

(29) Dhameliya, T. M.; Tiwari, R.; Banerjee, A.; Pancholia, S.; Sriram, D.; Panda, D.; Chakraborti, A. K. Benzo [d] thiazole-2-carbanilides as new anti-TB chemotypes: design, synthesis, biological evaluation, and structure-activity relationship. *Eur. J. Med. Chem.* **2018**, *155*, 364−380.

(30) Dhameliya, T. M.; Patel, K. I.; Tiwari, R.; Vagolu, S. K.; Panda, D.; Sriram, D.; Chakraborti, A. K. Design, synthesis, and biological evaluation of benzo [d] imidazole-2-carboxamides as new anti-TB agents. *Bioorg. Chem.* **20212021**, *107*, 104538.

(31) Marwaha, S.; Uvell, H.; Salin, O.; Lindgren, A. E.; Silver, J.; Elofsson, M.; Gylfe, Å. N-acylated derivatives of sulfamethoxazole and sulfafurazole inhibit intracellular growth of Chlamydia trachomatis. *Antimicrob. Agents Chemother.* **2014**, *58*, 2968−2971.

(32) Zuse, A.; Schmidt, P.; Baasner, S.; Böhm, K. J.; Müller, K.; Gerlach, M.; Günther, E. G.; Unger, E.; Prinz, H. Sulfonate derivatives of naphtho [2, 3-b] thiophen-4 (9 H)-one and 9 (10 H)-anthracenone as highly active antimicrotubule agents. Synthesis, antiproliferative activity, and inhibition of tubulin polymerization. *J. Med. Chem.* **2007**, *50*, 6059−6066.

(33) Mahapatra, M. K.; Kumar, R.; Kumar, M. Exploring sulfonate esters of 5-arylidene thiazolidine-2, 4-diones as PTP1B inhibitors with anti-hyperglycemic activity. *Med. Chem. Res.* **2018**, *27*, 476−487.

(34) Casini, A.; Scozzafava, A.; Mastrolorenzo, C. T.; Supuran, L. T. Sulfonamides and sulfonylated derivatives as anticancer agents. *Curr. Cancer Drug Targets* **2002**, *2*, 55−75.

(35) Bhagat, S.; Supriya, M.; Pathak, S.; Sriram, D.; Chakraborti, A. K. α-Sulfonamidophosphonates as new anti-mycobacterial chemotypes: Design, development of synthetic methodology, and biological evaluation. *Bioorg. Chem.* **2019**, *82*, 246−252.

(36) Ogemdi, I. K. A Review on the Properties and Uses of Paracetamol. *Int. J. Pharm. Chem.* **2019**, *5*, 31.

(37) Dennis, M. L.; Newman, J.; Dolezal, O.; Hattarki, M.; Surjadi, R. N.; Nuttall, S. D.; Pham, T.; Nebl, T.; Camerino, M.; Khoo, P. S.; Monahan, B. J.; Peat, T. S. Crystal structures of human ENPP1 in apo and bound forms. *Acta Crystallogr., Sect. D: Struct. Biol.* **2020**, *76*, 889−898.

(38) Belli, S. I.; Goding, J. W. Biochemical characterization of human PC-1, an enzyme possessing alkaline phosphodiesterase I and nucleotide pyrophosphatase activities. *Eur. J. Biochem.* **1994**, *226*, 433−443.

(39) Jin-Hua, P.; Goding, J. W.; Nakamura, H.; Sano, K. Molecular cloning and chromosomal localization of PD-Iβ (PDNP3), a new member of the human phosphodiesterase I genes. *Genomics* **1997**, *45*, 412−415.

(40) Kukulski, F.; Lévesque, S. A.; Lavoie, E. G.; Lecka, J.; Bigonnesse, F.; Knowles, A. F.; Robson, S. C.; Kirley, T. L.; Sévigny, J. Comparative hydrolysis of P2 receptor agonists by NTPDases 1, 2, 3 and 8. *Purinergic Signalling* **2005**, *1*, 193.

(41) Bradford, M. M. A rapid and sensitive method for the quantitation of microgram quantities of protein utilizing the principle of protein-dye binding. *Anal. Biochem.* **1976**, *72*, 248−254.

(42) Abdelazeem, A. H. A. M. H. A.; Gouda, M. F.; Omar, H. A.; Tolba, M. F. Design, synthesis and biological evaluation of novel diphenylthiazole-based cyclooxygenase inhibitors as potential anticancer agents. *Bioorg. Chem.* **2014**, *57*, 132−141.

(43) Gorelik, A.; Randriamihaja, A.; Illes, K.; Nagar, B. Structural basis for nucleotide recognition by the ectoenzyme CD 203c. *FEBS J.* **2018**, *285*, 2481−2494.

(44) MOE (Molecular Operating Environment). *Chemical Computing Group; CCG* version 2019.0201, 2019.

(45) *LeadIT version 2.3.2*; BioSolveIT GmbH: Sankt Augustin, Germany, 2017.

(46) *Dassault Systemes BIOVIA Discovery Studio Modeling Environment*; ReleaseDassault Systemes: San Diego, 2017.